https://doi.org/10.5194/acp-2022-644
Preprint. Discussion started: 4 October 2022

Atmospheric Chemistry and Physics Discussions

Impact of fossil and non-fossil sources on the molecular compositions of water soluble humic-like substance in $PM_{2.5}$ at a suburb site of Yangtze River Delta, China

Mengying Bao[1,2,3], Yan-Lin Zhang[1,2,*], Fang Cao[1,2], Yihang Hong[1,2], Yu-Chi Lin[1,2], Mingyuan Yu[1,2], Hongxing Jiang[4,5], Zhineng Cheng[4,5], Xiaoying Yang[1,2]

1 School of Applied Meteorology, Nanjing University of Information Science & Technology, Nanjing 210044, China.
2 Atmospheric Environment Center, Joint Laboratory for International Cooperation on Climate and Environmental Change, Ministry of Education (ILCEC), Nanjing University of Information Science & Technology, Nanjing 210044, China.
3 Huzhou Meteorological Administration, Huzhou 313300, China
4 State Key Laboratory of Organic Geochemistry and Guangdong province Key Laboratory of Environmental Protection and Resources Utilization, Guangzhou Institute of Geochemistry, Chinese Academy of Sciences, Guangzhou 510640, China.
5 CAS Center for Excellence in Deep Earth Science, Guangzhou 510640, China
Correspondence: Yan-Lin Zhang (dryanlinzhang@outlook.com)

Abstract

Atmospheric humic-like substances (HULIS) affect global radiation balance due to its strong light absorption at the ultraviolet wavelength. The potential sources and molecular compositions of water soluble HULIS at a suburb site of Yangtze River Delta from 2017 to 2018 were discussed based on the radiocarbon (^{14}C) analysis combining the Fourier Transform Ion Cyclotron Resonance Mass Spectrometry (FT-ICR MS) technique in this study. The ^{14}C results showed that the averaged non-fossil source contributions to HULIS were 39 ± 8 % and 36 ± 6 % in summer and winter, respectively, indicating that both the fossil and non-fossil sources played important roles in the formation of HULIS. The Van Krevelen diagrams obtained from the FT-ICR MS results showed that the proportions of tannins-like and carbohydrates-like groups were higher in summer, suggesting significant contribution of HULIS from biogenic secondary organic aerosols (SOA). The higher proportions of condensed aromatic structures in winter suggested the increasing anthropogenic emissions. Molecular composition analysis on the CHO, CHON, CHOS, and

https://doi.org/10.5194/acp-2022-644
Preprint. Discussion started: 4 October 2022

Atmospheric Chemistry and Physics Discussions

CHONS subgroups showed the relatively higher intensities of high O-containing macromolecular oligomers in CHO compounds in summer, further indicating stronger biogenic SOA formation in summer. High-intensity phenolic substances and flavonoids which were related to biomass burning and polycyclic aromatic hydrocarbons (PAHs) derivatives indicating fossil fuel combustion emissions were found in winter CHO compounds. Besides, two high-intensity CHO compounds containing condensed aromatic ring structures ($C_9H_6O_7$ and $C_{10}H_5O_8$) identified in summer and winter samples were similar to those from off-road engine samples, indicating that traffic emission was one of the important fossil sources of HULIS at the study site. The CHON compounds were mainly composed of organonitrates or nitro compounds with significant higher intensities in winter, which was associated to enhanced formation of organonitrates due to high NO_x in winter. However, the high-intensity CHON molecular formulas in summer were referring to N-heterocyclic aromatic compounds, which were produced from the atmospheric secondary processes involving reduced N species (e.g., ammonium). The S-containing compounds were mainly composed of organosulfates (OSs) derived from biogenic precursors, long-chain alkane and aromatic hydrocarbon, further illustrating the mixed sources of HULIS and both important biogenic and anthropogenic source contributions to HULIS at the study site. These findings add to our understanding of the interaction between the sources and the molecular compositions of atmospheric HULIS.

1. Introduction

Atmospheric humic-like substances (HULIS) have been observed worldwide and can be produced from primary combustion of biomass, fossil fuel, as well as various secondary processes such as photochemical processes of volatile organic compounds (VOCs) and heterogeneous reactions of organic aerosols in the atmosphere (Kuang et al., 2015; Li et al., 2019; Ma et al., 2018; Sun et al., 2021). As important component of brown caron (BrC) aerosols, HULIS species have been widely reported to have a great impact on global radiative budget, contributing to 20-40% of the direct radiative forcing caused by light absorbing aerosols due to its light absorption at the ultraviolet wavelength (Chung et al., 2012; Zhang et al., 2017; Zhang et al., 2020; Wang et al., 2018b). HULIS are a highly complex mixture of polar organic compounds composed of aromatic and hydrophobic aliphatic structures containing carboxyl, carbonyl, and hydroxyl function groups (Zheng et al., 2013; Graber and Rudich, 2006). During the atmospheric secondary oxidation

https://doi.org/10.5194/acp-2022-644
Preprint. Discussion started: 4 October 2022


Atmospheric Chemistry and Physics Discussions

processes, the substitutions of hydrophilic functional groups produced aerosol hygroscopicity (Huo et al., 2021; Jiang et al., 2020). Polycarboxylic acids in HULIS are surface-active and play an important role in the cloud condensation nuclei (CCN) activity (Tsui and McNeill, 2018). N-base compounds can promote the generation of atmospheric reactive oxygen species (ROS) which have a great impact on human health (Wang et al., 2017b; De Haan et al., 2018; Song et al., 2022). Identifying the molecular compositions of HULIS is a challenge due to complex mixtures contained in HULIS and can help to a better understanding of the processes involving organic compounds in atmosphere (Noziere et al., 2015; Laskin et al., 2018).

The Fourier-Transform Ion Cyclotron Resonance Mass Spectrometry (FT-ICR MS) coupled with electrospray ionization (ESI) ion source have been widely used in identifying the chemical structure of HULIS, providing high mass accuracy and can determine molecular formulas from mixed compounds (Chen et al., 2016; Wang et al., 2019b; Lin et al., 2012a; Jiang et al., 2020). Typical molecular formulas composed of C, H, and O atoms in HULIS were observed being abundant in carboxylic acids, lingin-derived products, and polycyclic aromatic hydrocarbons (PAHs) or their derivatives (Lin et al., 2012a; Sun et al., 2021; Jiang et al., 2020; Huo et al., 2021; Song et al., 2018). In addition, the HULIS formation of N and S containing precursors were also widely detected. The N-containing compounds such as nitroaromatics were important chromophores in HULIS in aged biomass burning organic aerosols (BBOA), as well as in ambient aerosols influenced by biomass burning (BB), while reduced N compounds such as N-heterocyclic aromatic compounds were found to be important chromophores in fresh BBOA (Wang et al., 2019b; Song et al., 2022; Jiang et al., 2020; Wang et al., 2017b). Recent laboratory simulation experiments showed that the photooxidation of various anthropogenic VOCs (e.g., naphthalene, benzene, toluene, and ethylbenzene) would be promoted under high NO_x condition, producing strongly light absorbing nitroaromatics (Yang et al., 2022; Aiona et al., 2018; Siemens et al., 2022; Xie et al., 2017). Otherwise, nighttime oxidation of biogenic or anthropogenic VOCs, such as benzene/toluene, isoprene (C_5H_8) and monoterpenes ($C_{10}H_{16}$) by NO_3 radicals lead to substantial organonitrates formation, where the VOCs oxidation is strongly affected by NO_x (He et al., 2021; Shen et al., 2021; Wang et al., 2020; Zheng et al., 2021).

The organosulfates (OSs) and nitrooxy organosulfates (nitrooxy-OSs) have also been found to widely exist in HULIS in different atmospheric environment (Lin et al., 2012b; Lin et al., 2012a; Sun et al., 2021). Field study and laboratory smog chamber experiments have confirmed that OSs

https://doi.org/10.5194/acp-2022-644
Preprint. Discussion started: 4 October 2022

Atmospheric Chemistry and Physics Discussions

and nitrooxy-OSs in the atmosphere mainly come from the O_3, OH, or NO_3 oxidation of biogenic VOCs such as isoprene, α/β-pinene as well as aromatic hydrocarbon in the presence of H_2SO_4/SO_2 (Surratt et al., 2008; Glasius et al., 2021; Yang et al., 2020; Lin et al., 2012b; Huang et al., 2020). Coal combustions were found to be important sources of the aromatic OSs and nitrooxy-OSs in HULIS (Song et al., 2018). Besides, the long-chain alkanes were found to be important precursor of OSs in atmospheric aerosol samples from urban area which was related to vehicle emissions (Wang et al., 2019a; Tao et al., 2014).

Nanjing is one of the main cities in the Yangtze River Delta (YRD), which is one of the most developed areas in China. Previous study reported by our laboratory have found significant HULIS formation at Nanjing, China influenced by both biogenic and anthropogenic emissions (Bao et al., 2022). The molecular compositions of water soluble HULIS isolated from $PM_{2.5}$ samples collected in summertime and wintertime from 2017 to 2018 at Nanjing, China, were investigated combining the FT-ICR MS and radiocarbon (^{14}C) analysis. We aim to obtain the molecular characteristic differences of water soluble HULIS in summertime and wintertime and to get a better understanding of the influence of different sources on the molecular compositions of HULIS.

2. Materials and methods

2.1 Sample collection

The 24 h $PM_{2.5}$ samples were collected on the roof of Wende building, which was about 21 m height from the ground at Nanjing University of Information Science and Technology (32.2° N, 118.7° E) using a high-volume sampler (KC-1000, Qingdao, China) at a flow rate of 300 L min^{-1}. The study site was located at the north suburb area of Nanjing, adjacent to G205 State Road and surrounded by an industrial park and residential area. Generally, the study site was affected by human activity, industrial emission, and traffic emission. The sample collection was conducted in summer from 12 August 2017 to 26 August 2017 and in winter from 31 December 2017 to 31 January 2018. A heavy haze event occurred from 31 December 2017 to 3 January 2018, thus the sample frequency was adjusted to 2 h in daytime and 8 h in nighttime. Field blank filters were performed before and after sample collection for each season. More details about the sample collection can be found in previous research reported by our laboratory (Bao et al., 2022). The air pollutants data were provided by China National Environmental Monitoring Centre. Twelve samples were selected for further chemical analysis and the details about the sample selection are described in Section 3.1 in this study.

https://doi.org/10.5194/acp-2022-644
Preprint. Discussion started: 4 October 2022


Atmospheric Chemistry and Physics Discussions

125 2.2 Chemical analysis

126 The solid phase extraction (SPE) was performed to isolate the water soluble HULIS in this
127 study and the carbon fraction in HULIS (HULIS-C) were determinated using a total carbon
128 analyzer (Shimadzu-TOC-VCPH, Shimadzu, Japan) with standard deviation of reproducibility test
129 less than 3.5% and detection limit of 0.14 μg C m^{-3}. The mass concentrations of levoglucosan were
130 measured using an ion chromatography (Dionex ICS-5000+, ThermoFisher Scientific, USA) and
131 the details of the methods have been described previously (Liu et al., 2019). All data were blank
132 corrected in this study. More details about the HULIS isolation and measurement have been
133 described in (Bao et al., 2022).

134 2.3 Radiocarbon analysis

135 For the radiocarbon measurement of the HULIS samples, the organic solvents were firstly
136 evaporated under a gentle flow of ultrapure N_2 for 30-40 minutes in tin cups. After that, the tin
137 cups were wrapped into balls and more than 50 μg of carbon from the HULIS samples was
138 combusted into CO_2 using an elemental analyzer (EA, model vario micro, elemental, Germany),
139 then reduced into graphite targets for ^{14}C determination at the State Key Laboratory of Organic
140 Geochemistry, Guangzhou Institute of Geochemistry, Guangzhou, China (Jiang et al., 2020).
141 Detailed descriptions of the ^{14}C data processing can be found in previous study (Mo et al., 2018).
142 Briefly, the ^{14}C values were expressed as the modern carbon (f_m) fraction after correcting for the
143 $\delta^{13}C$ fractionation. The f_m was converted into non-fossil carbon (f_{nf}) fraction with the correction
144 factor of 1.06±0.07 based on the long-term time series of $^{14}CO_2$ sampled at the background station
145 in this study (Levin et al., 2013; Levin and Kromer, 2004). No field blank correction was
146 performed for the carbon isotope analysis since the carbon content in the field blanks was
147 negligible.

148 2.4 High-resolution FT-ICR MS analysis

149 The ultrahigh resolution mass spectra of the HULIS samples were obtained through a SolariX
150 XR FT-ICR MS (Bruker Daltonics, GmbH, Bremen, Germany) equipped with a 9.4 T
151 superconducting magnet (Gamry Instruments, Warminster, USA) and a Paracell analyzer cell
152 (Brucker Daltonik GmbH, Bremen, Germany) in the negative ESI mode. The detection mass range
153 was set as m/z 150 to 800 and the ion accumulation time was set as 0.65 s. A total of 100 continuous
154 4M transient data points were superposed to enhance the signal to noise ratio and dynamic range.
155 The mass spectrum was externally calibrated with a standard solution of arginine and internal

https://doi.org/10.5194/acp-2022-644
Preprint. Discussion started: 4 October 2022


Atmospheric Chemistry and Physics Discussions

recalibration was performed using typical O_6S_1 chemical species in DataAnalysis ver. 4.4 software (Bruker Daltonics) (Mo et al., 2018; Tang et al., 2020; Jiang et al., 2020). Field blank filters were analyzed as same as the samples and all the sample data were blank corrected. More details about the data processing can be found in Text S1 in the supporting information.

3. Results and discussion

3.1 General temporal characteristics during the sampling periods

Figure 1 displays the temporal variations of non-fossil contributions to HULIS-C, the mass concentrations of HULIS-C, levoglucosan, NO_3^-, SO_4^{2-}, NH_4^+, SO_2, NO_2, and $PM_{2.5}$, as well as the relative humidity and temperature during the study periods corresponding to the 12 samples. The 12 samples were named as S1-S6 and W1-W6 in chronological order in this study. The averaged mass concentrations of $PM_{2.5}$ in summer and winter during the selected periods were 21.05 ± 8.05 μg m^{-3} and 445.67 ± 275.00 μg m^{-3}, respectively, indicating the serious pollution level in winter. The daily $PM_{2.5}$ mass concentrations in summer were all below the daily averaged Chinese National Ambient Air Quality Standard (NAAQS) of 35 μg m^{-3} for the first grade, while the daily $PM_{2.5}$ mass concentrations in winter all exceeded the daily averaged NAAQS of 35 μg m^{-3} for the first grade, of which the $PM_{2.5}$ mass concentrations of W1-W3 and W6 exceeded 200 μg m^{-3}.

As shown in Fig. 1, the mass concentrations of HULIS-C, levoglucosan, water soluble secondary inorganic aerosols (SIA), and air pollutants showed similar trends in winter, suggesting the influence of BB and anthropogenic emissions in winter (Wu et al., 2019b). Significant increasing of the levoglucosan and HULIS-C mass concentrations were found from 31 December 2017 to 1 January 2018, corresponding to the W1-W3 samples, indicating the BB impact during the periods. The maximum of the levoglucosan and HULIS-C mass concentrations were 552.79 μg m^{-3} and 7.40 μg m^{-3}, respectively. Despite the higher levoglucosan mass concentrations in the W1-W3 samples, the radiocarbon analysis results showed that the f_{nf} of HULIS-C ranged from 30 % to 50 % with an average contribution of 39 ± 8 % in summer and ranged from 32 % to 48 % with an average contribution of 36 ± 6 % in winter, indicating that both fossil and non-fossil sources played important roles in the formation of HULIS at the study site. There were other emission sources of HULIS in winter other than BB. Figure S1 shows the 48 h back trajectories of each sample during the selected periods. The study site was affected by the clean air masses from the ocean in summer and the air masses mainly from the northern heating cities in winter, suggesting the coal combustion contributions to HULIS in winter.

https://doi.org/10.5194/acp-2022-644
Preprint. Discussion started: 4 October 2022


Atmospheric Chemistry and Physics Discussions

187 3.2 Mass spectra and molecular formula assignments

188 Figure S2 and S3 shows the negative ion ESI FT-ICR mass spectra of HULIS in summer and
189 winter, respectively. The molecular formulas listed are some of the top ten molecular formulas.
190 Thousands of peaks are present in the spectra in the range from m/z 150 to m/z 600 and the most
191 intense ion peaks are those in the range m/z 200-400 in summer and m/z 150-350 in winter. Our
192 results are similar to those found for the ultrahigh resolution mass spectra of water-soluble organic
193 compounds in particles produced from BB, coal combustion, vehicle exhaust emissions, as well as
194 in ambient aerosols and cloud water samples (Tang et al., 2020; Sun et al., 2021; Song et al., 2018;
195 Song et al., 2019; Bianco et al., 2018). In this study, the assigned molecular formulas were
196 classified into the following four main subgroups based on their elemental compositions: CHO
197 (compounds containing only C, H, and O), CHON (compounds containing C, H, O and N), CHOS
198 (compounds containing C, H, O, and S), and CHONS (compounds containing C, H, O, N, and S).
199 As shown in Fig. 2, the proportions of the four subgroups accounted for the overall formulas
200 followed as CHO (20 %-27 %), CHON (28 %-43 %), CHOS (19 %-26 %), and CHONS (16 %-
201 26 %) in summer, respectively and CHO (15 %-19 %), CHON (30 %-40 %), CHOS (21 %-32 %),
202 and CHONS (20 %-29 %) in winter, respectively. The average proportions of the CHO, CHON,
203 CHOS, and CHONS compounds in summer were 22 ± 3 %, 36 ± 5 %, 22 ± 3 %, and 20 ± 4 %,
204 respectively. The average proportions of the four subgroups in winter were 17 ± 2 %, 32 ± 4 %,
205 24 ± 3 %, and 27 ± 4 %, respectively. The CHON groups were the major components of molecular
206 formulas. Notably, the contributions of S-containing compounds (CHOS and CHONS groups)
207 increased in winter which might be related to the polluted air masses transported from the northern
208 heating cities with increasing coal combustions emissions in winter (Song et al., 2018).

209 Table S1 and S2 displays the composition characteristics of atmospheric HULIS in the
210 summer and winter samples, including the relative intensity weighted average values of number,
211 molecular weight (MW_w), elemental ratios (O/C_w and H/C_w), double-bond equivalent (DBE_w),
212 aromaticity index (AI_w), and DBE/C_w. A total of 14387 and 15731 peaks were detected in the
213 summer and winter samples, respectively. The O/C and H/C ratios are commonly calculated to
214 evaluate the oxidation degree and saturation degree of the compounds, respectively (Ning et al.,
215 2022). The O/C_w values were in a range of 0.61-0.80 with an average value of 0.71 ± 0.07 for
216 summer samples and in a range of 0.59-0.67 with an average value of 0.62 ± 0.03 for winter
217 samples, respectively. The higher oxidation degree of summer samples than winter samples

https://doi.org/10.5194/acp-2022-644
Preprint. Discussion started: 4 October 2022


Atmospheric Chemistry and Physics Discussions

indicated stronger secondary HULIS formation in summer. The H/C_w values were in a range of 1.38-1.46 with an average value of 1.42 ± 0.03 for summer samples and in a range of 1.33-1.41 with an average value of 1.36 ± 0.04 for winter samples, respectively. The O/C_w and H/C_w of each molecular subgroup followed a changing trend of CHO < CHON < CHOS < CHONS compounds. Most of the S-containing compounds had a O/C value ≥0.7, suggesting the large amounts of highly oxidized OSs in S-containing compounds which contained various functional groups and were mainly from the photochemical oxidation of biogenic or anthropogenic volatile organic compounds (VOCs) (Mutzel et al., 2015). The DBE values were calculated to describe the degree of unsaturation of compounds and restricted the assigned molecular formulas with unreasonably high or low number of rings or double bonds (Kroll et al., 2011). The higher DBE_w and DBE/C_w values of CHO and CHON compounds were found in this study.

Considering that double bonds can be formed by heteroatoms especially O atoms, whereas make no contributions to the aromaticity of the compounds, AI_w was calculated to supplement the DBE results (Song et al., 2018; Ning et al., 2019). AI_w can eliminate the contribution of O, N, and S atoms to the C=C double bond density of molecules. The AI_w values of different compounds groups in HULIS presented the changing trends: AI_w (CHONS) > AI_w (CHON) > AI_w (CHO) > AI_w (CHOS) in summer and AI_w (CHON) > AI_w (CHO) > AI_w (CHONS) > AI_w (CHOS) in winter, respectively. The formulas can be classified into three parts based on AI values proposed by previous studies: aliphatic (AI =0), olefinic (0< AI ≤0.5) and aromatic (AI >0.5) (Koch and Dittmar, 2006). As shown in Fig. S4 and S5, the aliphatic were the main components of S-containing compounds in this study and the olefinic and aromatic were the main components of CHO and CHON compounds. Furthermore, the aromatic proportion of CHO and CHON compounds significantly increased in winter, suggesting the increasing anthropogenic emissions in winter.

3.3 Comparative analysis using Van Krevelen diagrams

In this study, the Van Krevelen diagrams (Fig. 3) were constructed to display the molecular composition and categorical distribution of the collected samples (Noziere et al., 2015; Patriarca et al., 2018; Li et al., 2022). According to the elemental ratios (O/C and H/C ratios) and AI values, seven major compound classes were classified, including lipids-like species, lignins-like species, proteins-like species, tannins-like species, carbohydrates-like species, condensed aromatics structure, and unsaturated hydrocarbons (Table S3). The Van Krevelen diagrams showed similar distributions in the 12 samples. The CHO and CHON compounds located in the lower left area

https://doi.org/10.5194/acp-2022-644
Preprint. Discussion started: 4 October 2022


Atmospheric Chemistry and Physics Discussions

and the S-containing compounds located in the upper light area with higher O/C and H/C ratios, indicating a higher degree of oxidation and saturation. The condensed aromatic structure mainly consisted in CHO and CHON compounds, further suggesting the influence of anthropogenic emissions on the formation of CHO and CHON compounds.

Figure 4 presents the averaged relative contributions of the number of molecular formulas from the seven categories in summer and winter samples, respectively. Lignins-like species accounted for the highest proportion of CHO compounds with average contributions of 58 % and 61 % in summer and winter, respectively, followed by CHON compounds with average contributions of 48 % and 57 % in summer and winter, respectively. Lignins are mainly composed of carboxyl groups, alicyclic rings, aromatic rings, and other O-containing groups. Previous studies have reported that lignin was a complex phenolic polymer which usually came from direct biological emissions or combustions of biofuel (Ning et al., 2019; Boreddy et al., 2021; Sun et al., 2021). Lignins pyrolysis products and other lignins derived molecules have been shown to be oxidized into light absorbing BrC chromophore under certain conditions (Fleming et al., 2020).

Tannins-like species accounted for 21 %, 27 %, 23 %, and 30 % of CHO, CHON, CHOS, and CHONS compounds, respectively in summer which were higher than those in winter with contributions of 13 %, 16 %, 16 %, and 23 % to CHO, CHON, CHOS, and CHONS compounds, respectively. Tannins-like species are a series of polyphenolic compounds containing hydroxyls and carboxylic groups which have been widely reported in fogs, cloud water and aerosol samples, attributing to highly oxidized organic compounds such as OSs or nitrooxy-OSs produced from the nighttime chemistry between the biogenic VOCs with the NO_3 (Altieri et al., 2009; Bianco et al., 2018; Ning et al., 2019; Altieri et al., 2008; Shen et al., 2021). Carbohydrates-like species which contain monosaccharide, alditols, and anhydrosugars mainly consisted in CHONS compounds which also had a relative higher proportion of 33 % in summer than that of 29 % in winter (Sun et al., 2021). $C_{10}H_{16}NO_{7\text{-}9}S$, as monoterpene nitrooxy-OSs, showing high relative intensities, were typical carbohydrates-like species detected in this study which represented biogenic secondary organic aerosols (SOA) (Ning et al., 2019; Surratt et al., 2008; Wang et al., 2020). Both the higher proportions of tannins-like and carbohydrates-like classes in summer indicated stronger biogenic SOA formation in this study.

Proteins-like classes mainly consisted in CHOS compounds with average proportions of 29 % and 38 % in summer and winter, respectively. Proteins contain peptide-like structures formed by

https://doi.org/10.5194/acp-2022-644
Preprint. Discussion started: 4 October 2022


Atmospheric Chemistry and Physics Discussions

dehydration with different kinds of amino acids and consist of short chains of amino acid residues (Bianco et al., 2018). These compounds are associated with photochemical oxidation processing in aerosols, thus resulting in the significant formation of OSs from biogenic or anthropogenic precursors in this study (Bigg and Leck, 2008).

Higher condensed aromatics were detected in winter with average proportions of 14 % in CHO compounds and 8 % in CHON compounds, respectively which were 2-2.5 times of those in summer. Condensed aromatics are important components of PAHs which usually emitted from incomplete combustion of fossil fuels (Ma et al., 2020). The increase of the proportion of condensed aromatics in winter indicated the stronger influence of anthropogenic sources on HULIS formation. The unsaturated hydrocarbons and lipids-like species showed the lowest molecular number percentage of less than 1 % in this study. Previous studies have shown that the lipids-like species were the main components of water insoluble organic compounds in aerosols and could be attributed to monocarboxylic acids (Ning et al., 2022; Wozniak et al., 2008).

In summary, both the summer and winter samples were mainly composed of compounds from biogenic origins (lignins-like, tannins-like, proteins-like, and carbohydrates-like species). It is noted that ESI ionization technology is more sensitive for the identification of polar compounds. Therefore, the low polar or nonpolar compounds, such as PAHs or their derivatives from fossil sources, were probably underestimated in this study (Jiang et al., 2014; Lin et al., 2018).

3.4 Molecular composition of HULIS

3.4.1 Molecular characteristics of CHO compounds

The O/C_w and H/C_w ratios for the CHO compounds were 0.45-0.56 and 1.15-1.30 for the summer samples and 0.42-0.48 and 0.90-1.02 for the winter samples (Table S1 and S2). The summer samples showed higher oxidation degree and saturation degree. We firstly plotted the Van Krevelen diagrams of the four molecular subgroups showing relative intensities for all the 12 samples and similar distributions of the high-intensity compounds were found in the 6 summer samples and the 6 winter samples, respectively. Then we combined all the data in summer and winter, respectively. As shown in Fig. 5a and 5d, the CHO compounds in summer with high relative abundance were located at the area within $0.2 \leq O/C \leq 1.0$ and $1.0 \leq H/C \leq 1.7$, mainly including lignins-like species and tannins-like species which were closely related to biogenic emissions. On the contrary, the condensed aromatics showed high relative abundance in winter, suggesting the obvious different sources of HULIS in summer and winter. The DBE values

https://doi.org/10.5194/acp-2022-644
Preprint. Discussion started: 4 October 2022


Atmospheric Chemistry and Physics Discussions

311 increased with the increasing of the C numbers (Fig. 5b and 5e). The high-intensity CHO
312 compounds in HULIS had DBE values between 3-7 with C numbers from 10 to 20 for summer
313 samples. In winter, the high-intensity CHO compounds had DBE values between 7-11 with C
314 numbers from 5 to 15. As mentioned above, the aromatic (AI >0.5) proportion of CHO compounds
315 significantly increased in winter, the higher DBE values in winter further indicated the consists of
316 more highly unsaturated aromatic compounds which reflected the anthropogenic emissions.
317 The CHO compounds were classified according to the number of oxygen atoms to evaluate
318 the oxygen content. As shown in Fig. 5c and 5f, the high-intensity CHO compounds with 6-11
319 oxygen atom were detected in summer, such as $C_{15}H_{24}O_6$, $C_{15}H_{22}O_{10}$, $C_{18}H_{26}O_8$, and $C_{18}H_{26}O_9$,
320 these highly oxygenated organic molecules with high molecular weight have also been detected in
321 laboratory α-pinene ozonolysis SOA (Pospisilova et al., 2020). We further classified the CHO
322 compounds by different carbon atom numbers. As shown in Fig. S6, the C_{17}-C_{22} compounds were
323 the main components of the CHO compounds, accounting for more than 50 % of the total number
324 of CHO molecular formulas in both summer and winter seasons. However, the total relative
325 intensities of the CHO compounds in summer were significantly higher than those in winter, of
326 which the C_{23}-C_{26} and C_{27}-C_{32} compounds were enrich in summer. These high molecular weight
327 compounds were probably oligomers formed from various biogenic precursors, such as isoprene,
328 sesquiterpene, and monoterpene (Daellenbach et al., 2019; Berndt et al., 2018). The high intensities
329 of these compounds in summer further indicated the stronger biogenic SOA formation in summer
330 compared with that in winter.
331 High-intensity CHO compounds with 4-9 oxygen atom were detected in winter (Fig. 5c) of
332 which the $C_{14}H_{10}O_4$ formula with a DBE value of 10 appeared the highest intensity, which was
333 probable functional PAHs and have been reported in HULIS from coal combustion smoke particles
334 (Song et al., 2019). As shown in Fig. S2 and S3, the $C_{14}H_{10}O_4$ formula appeared high intensity in
335 all the winter samples, providing the evidence of coal combustion emissions in winter. Some other
336 high-intensity compounds in winter, such as $C_{14}H_8O_4$ and $C_{14}H_8O_5$ both with DBE values of 11,
337 and $C_{13}H_8O_2$, $C_{13}H_8O_5$, and $C_{13}H_8O_6$ with DBE values of 10, might refer to hydroxyl substitutions
338 derived from anthracenedione and xanthone, respectively, which have been reported in secondary
339 wood combustion products (Bruns et al., 2015). $C_{15}H_{10}O_6$, $C_{15}H_8O_6$, and $C_{16}H_{12}O_7$ which had
340 DBE values of 11, 12, and 11, respectively, might be flavonoids which had flavone backbone, the
341 key structure of plant pigments, widely existing in plants in nature and could be important sources

https://doi.org/10.5194/acp-2022-644
Preprint. Discussion started: 4 October 2022


Atmospheric Chemistry and Physics Discussions

of BrC chromophores in aged BBOA (Fleming et al., 2020; Lin et al., 2016; Huang et al., 2021). Phenolic substances derived from phenol, guaiacol, and syringol are also widely existed in BBOA, usually from the pyrolysis of lignins in wood, which also play an important role in aqueous-phase SOA formation (Boreddy et al., 2021). For instance, $C_{13}H_{10}O_3$ and $C_{13}H_{10}O_5$ are guaiacol derivatives, $C_{15}H_{16}O_8$ are syringol derivatives and $C_{18}H_{14}O_6$ and $C_{18}H_{14}O_7$ are phenol derivatives (Sun et al., 2021). As shown in Fig. S7, the relative intensities of the CHO compounds mentioned above produced from BB were found to have similar trends with the mass concentrations of levoglucosan, which were significantly higher in W1-W3 samples, corresponding to the BB period from 31 December 2017 to 1 January 2018, providing the evidence of BB influence on HULIS formation in winter.

It is noted that the top compounds $C_9H_6O_7$ and $C_{10}H_6O_8$ were detected both in the summer and winter samples (Fig. S2 and S3), which had DBE values of 7 and 8, respectively, containing abundant condensed aromatic ring structures with high O numbers. Their peaks were also detected in the HFO (heavy-fuel-oil)-fueled off-road engine samples reported before, suggesting the traffic emission contributions to HULIS (Cui et al., 2019). This supported the radiocarbon analysis results in this study and gave further information that the traffic emissions were important fossil sources in both summer and winter seasons.

3.4.2 Molecular characteristics of CHON compounds

The O/C_w of CHON compounds in summer and winter were 0.57-0.71 and 0.52-0.56, respectively, while the H/C_w were 1.20-1.32 and 1.00-1.11, respectively (Table S1 and S2). Compared with the summer CHON compounds, the winter CHON compounds presented significant higher ion abundance (Fig. 6a and 6d). The most abundant CHON subgroups had DBE values of 4-7 and 3-10 in summer and winter, respectively (Fig. 6b and 6e). Similar with CHO compounds, the higher DBE values of high-intensity CHON compounds in HULIS in winter indicated a high prevalence of double bonds or ring structures. According to the N and O number, the CHON compounds were classified into N_1O_x (N_1O_1-N_1O_{15}) and N_2O_x (N_2O_2-N_2O_{14}) subgroups in summer and N_1O_x (N_1O_1-N_1O_{12}) and N_2O_x (N_2O_2-N_2O_{12}) subgroups in winter, respectively (Fig. 6c and 6f). $NO_{8\text{-}12}$ and $NO_{6\text{-}9}$ compounds were most enriched subgroups in summer and winter, respectively. More oxygen-enriched CHON compounds containing O number above 9 were detected in summer, implying the higher oxidation degree for summer samples. In addition, the N_1O_x were both the major compounds represented average of 64 ± 4 % and 61 ± 6 % of the CHON

https://doi.org/10.5194/acp-2022-644
Preprint. Discussion started: 4 October 2022


Atmospheric Chemistry and Physics Discussions

molecular formulas in summer and winter, respectively, indicating the presence of more single nitro/amino substituents in CHON compounds in this study.

Among the CHON compounds, 95 ± 1 % and 86 ± 3 % CHON compounds had O/N values ≥3 in summer and winter, respectively in this study, indicating these compounds contained large amounts of oxidized nitrogen functional groups such as nitro compounds (-NO_2) and/or organonitrates (-ONO_2) and excess oxygen atoms indicated the existence of other oxygen-containing functional groups (Laskin et al., 2009). The organonitrates formation from NO_3 oxidation of biogenic or anthropogenic VOCs can affect the interactions between anthropogenic and natural emissions (He et al., 2021; Shen et al., 2021; Wang et al., 2020). Organonitrates were found to be important species contributing to SOA formation in polluted urban environment, which were enhanced under high NO_x level (Zheng et al., 2021). The significant higher relative intensities of CHON compounds in winter indicated that the high NO_x environment in winter promoted the formation of organonitrates and highlighted the importance of orgnonitrates for SOA control in polluted environment.

Furthermore, we found that the increase of the relative abundance of CHON compounds in winter was particularly significant in W1-W3 samples (Fig. S2 and S3), corresponding to the BB episode. Phenols produced from the pyrolysis of lignins can react with NO_3 radicals in the atmosphere, producing nitrophenols, which have been shown to be important BrC chromophore in BBOA (Wang et al., 2017b; Lin et al., 2016; Cai et al., 2020). It was reported that the gas-phase reactions of NO_3 radicals with phenolic substances took place at least 4 orders of magnitude faster than those with aromatic hydrocarbon and even faster in the aqueous phase (Lin et al., 2017). Among the top CHON compounds with high relative abundance in W1-W3 samples, such as $C_6H_4N_2O_6$ and $C_7H_6N_2O_6$ with DBE values of 5 and 6, respectively, were refer to nitrophenols containing one or two nitrogen-containing functional groups, which have been widely reported in aged BBOA, indicating the increasing of the CHON compounds relative intensity in W1-W3 samples were closely related to BB (Lin et al., 2017; Cai et al., 2020; Mohr et al., 2013; Kourtchev et al., 2016; Lin et al., 2016). Some other top CHON compounds in winter samples such as $C_9H_4NO_4$ and $C_{10}H_6NO_4$ with low O/C and H/C ratios most likely indicated the presence of condensed aromatic structures in the compounds. The $C_9H_4NO_4$ compounds were most likely emitted from vehicle emissions which have previously been reported (Cui et al., 2019).

https://doi.org/10.5194/acp-2022-644
Preprint. Discussion started: 4 October 2022


Atmospheric Chemistry and Physics Discussions

It is worth noting that some high-intensity CHON compounds with low O/C and H/C ratios were detected in summer samples in this study (Fig. 6a), which were closely related to aromatic compounds from anthropogenic emissions. The top compounds with molecular formulas of $C_8H_5N_2O_2$ and $C_{19}H_{11}N_2O_4$, which had O/N of 2 and 1, respectively, both were reduced N compounds referring to N-heterocyclic compounds. Previously study have found that the N-heterocyclic aromatic compounds can be formed through the aldehyde−ammonia reactions (De Haan et al., 2018; Zhang et al., 2022). This indicated the important role of reduced N species (e.g., ammonium) in the formation of anthropogenic SOA in summer.

3.4.3 Molecular characteristics of S-containing compounds (CHOS and CHONS compounds)

The O/C_w of CHOS compounds in summer and winter were 0.60-0.79 and 0.56-0.67, respectively, while the H/C_w were 1.50-1.54 and 1.53-1.72, respectively. The O/C_w of CHONS compounds in summer and winter were 0.82-1.01 and 0.76-0.94, respectively, while the H/C_w were 1.57-1.65 and 1.58-1.66, respectively (Table S1 and S2). As shown in Fig. 7a, 7d, 8a, and 8d, the high-intensity S-containing compounds in summer and winter were both located at the area where O/C >0.5 and H/C >1.5, respectively. In addition, the relative intensity of S-containing compounds increased with the O/C ratios, suggesting the S-containing compounds were highly oxidized. A small number of high-intensity S-containing compounds with O/C <1.0 and H/C <1.0 were also found in winter in this study, which might be related to OSs and nitrooxy-OSs produced from the oxidation of aromatic hydrocarbon. The CHOS compounds presenting high relative abundance were rich in $O_{6\text{-}9}S$ and $O_{5\text{-}7}S$ groups in summer and winter, respectively, of which the DBE values were all below 4. The CHONS compounds were rich in $O_{8\text{-}10}S$ and $O_{7\text{-}9}S$ groups in summer and winter, respectively, of which the DBE values were all below 6 (Fig. 7b, 7e, 7c, 7f, 8b, 8e, 8c, and 8f). Compared with those of the CHO and CHON compounds, the DBE values of S-containing compounds were significantly lower.

Among the S-containing compounds, more than 95 % of the CHOS, $CHON_1S$, and $CHON_2S$ formulas had O/S ratios greater than 4, 7, and 10, respectively, implying these compounds may contain organic sulfate functional groups ($-OSO_3$) or one or two organic nitrate groups ($-ONO_2$) and these compounds are more likely OSs or nitrooxy-OSs, presenting lower DBE values and higher O/C and H/C ratios (Table S5 and S6) (O'Brien et al., 2014). The high-intensity CHONS compounds observed in this study, such as $C_{10}H_{16}NO_{7\text{-}9}S$, $C_{10}H_{18}NO_{8\text{-}9}S$, $C_{10}H_{18}N_2O_{11}S$, and

https://doi.org/10.5194/acp-2022-644
Preprint. Discussion started: 4 October 2022


Atmospheric Chemistry and Physics Discussions

$C_9H_{14}NO_8S$ could be nitrooxy-OSs derived from limonene, α-terpinene, and monoterpene (Figure S2 and S3) (Sun et al., 2021; Bruggemann et al., 2020; Wang et al., 2020; Wang et al., 2018c).

The CHOS compounds with high intensity abundance, such as typical isoprene epoxydiols (IEPOX) derived OSs with molecular formulas of $C_5H_8O_7S$ and $C_5H_{10}O_7S$ were both detected in the summer and winter samples, of which the relative intensity of $C_5H_8O_7S$ were over 80 % in S1, S2, S5, and S6 samples, indicating the significant isoprene SOA formation in summer (Kourtchev et al., 2016; Kourtchev et al., 2013). The results were consistent with the previous research on the sources of HULIS based on positive matrix factorization (PMF) model reported by our laboratory (Bao et al., 2022). The monoterpenes derived OSs such as $C_8H_{14}O_6S$, $C_8H_{14}O_8S$, $C_{10}H_{18}O_8$, $C_{10}H_{14}O_6$, and $C_{11}H_{16}O_7$ were detected in both summer and winter samples in this study, which could refer to monoterpene-OSs derived from α-pinene, α-terpinene, and limonene (Wang et al., 2020). Moreover, OSs with high carbon numbers (C ≥14) such as $C_{14}H_{22}O_7S$, $C_{14}H_{22}O_8S$, $C_{14}H_{24}O_7S$, $C_{15}H_{26}O_7S$, $C_{15}H_{24}O_7S$, $C_{15}H_{24}O_8S$, and $C_{16}H_{28}O_7S$ were also observed in both summer and winter samples. Long-chain alkanes emitted from vehicle emissions might be precursors of these OSs which was consistent with the molecular structures of OSs collected in urban areas affected by traffic emissions such as Shanghai, Los Angeles, and Beijing (Wang et al., 2019a; Tao et al., 2014; Wang et al., 2016). The aromatic OSs such as naphthalene derived OSs with molecular formulas of $C_{10}H_{10}O_6S$, $C_{10}H_{10}O_7S$, and $C_{10}H_{12}O_7S$, 2-methylnaphthalene derived OSs with molecular formulas of $C_9H_{12}O_6S$, $C_{11}H_{12}O_7S$, and $C_{11}H_{14}O_7S$, and hydroxybenzene derived OSs with molecular formulas of $C_6H_6O_5S$ were also observed in this study (Qi et al., 2021; Riva et al., 2015; Blair et al., 2017). Figure S8 further displays the ternary plot of the relative intensities of OSs from biogenic precursors (e.g., isoprene and monoterpenes), long-chain alkanes and aromatic hydrocarbon. As shown in Fig. S8, the biogenic OSs and long-chain alkanes OSs formation were comparable in summer and winter, demonstrating both biogenic and anthropogenic emission contributions to HULIS. The aromatic OSs presented higher relative intensities in winter, further indicating the increasing anthropogenic emissions in winter. The presence of long-chain alkanes derived OSs in both summer and winter seasons provided another evidence that the traffic emission was one of the important fossil sources of HULIS in this study.

3.5 Comparison with organic compounds in source and atmospheric aerosol samples

The O/C and H/C ratios of water soluble HULIS in this study were compared with those of water soluble organic compounds reported in source samples from BB, coal combustions, and

https://doi.org/10.5194/acp-2022-644
Preprint. Discussion started: 4 October 2022


Atmospheric Chemistry and Physics Discussions

vehicle emissions (Tang et al., 2020; Song et al., 2018; Cui et al., 2019; Song et al., 2019), cloud water samples (Bianco et al., 2018; Zhao et al., 2013), rainwater samples (Altieri et al., 2009), fog samples (Brege et al., 2018), as well as aerosol samples collected in Beijing (Jang et al., 2020; Wu et al., 2019a; Wang et al., 2018a), Tianjin (Han et al., 2022), Baoding (Sun et al., 2021), Shanghai (Wang et al., 2017a), Guangzhou (Jiang et al., 2021), respectively in China, Mainz (Wang et al., 2018a), Cork city (Kourtchev et al., 2014), and Bologna (Brege et al., 2018), respectively in Europe, and Bakersfield (O'Brien et al., 2014) and Virginia (Willoughby et al., 2014), respectively in the United States (Fig. 9). The O/C ratios were obviously higher than those detected in primary BB, coal combustion, and vehicle emission samples. The H/C ratios of the CHO and CHON compounds were comparable with the source samples, indicating the organics in HULIS experienced atmospheric secondary process and the mixed sources of HULIS in this study. The H/C ratios of the S-containing compounds were much higher than those of source samples which could be attributed to the significant organosulfates formation in the atmosphere.

The O/C ratios reported in this study were also higher than those reported in aerosol samples in urban area in China, further indicating the serious secondary pollution at Nanjing, China. Among the CHO and CHON compounds, we found that the highest H/C ratio values were observed in the southern city of Guangzhou, followed by those in Nanjing and Shanghai, and the lowest values were observed in the northern cities such as Beijing, Tianjin, and Baoding, indicating the higher unsaturation degree of the aerosol samples collected from the northern heating cities, which were also considered as the heavy industrial region in China. The higher H/C ratios of aerosol samples collected in Europe and the United States indicated the less anthropogenic emissions such as industrial emissions from those areas.

4. Conclusions

This study focuses on the sources and molecular characteristics differences of water soluble HULIS in summertime and wintertime from 2017 to 2018 at a suburb site of the YRD, China based on the radiocarbon analysis and FT-ICR MS measurement with ESI ion source in negative mode. The carbon isotope analysis results highlight both important fossil and non-fossil source contributions to HULIS at the study site. A total of 14387 and 15731 peaks were detected in the summer and winter samples, respectively based on the FT-ICR MS results. The assigned molecular formulas were classified into CHO, CHON, CHOS, and CHONS subgroups according to their elemental compositions. The Van Krevelen diagrams showed that more tannins-like and

https://doi.org/10.5194/acp-2022-644
Preprint. Discussion started: 4 October 2022


Atmospheric Chemistry and Physics Discussions

carbohydrates-like species were detected in summer indicating biogenic SOA formation. Whereas more compounds containing condensed aromatic structures were detected in winter which were derived from anthropogenic emissions. The total relative intensity of CHO compounds in summer were significantly higher than those in winter, containing lots of macromolecular oligomers derived from biogenic precursors. The high-intensity CHO compounds in winter were mainly aromatic compounds such as phenolic substances and flavonoids which were related to aged BBOA and oxidized PAHs most probably from fossil fuel combustion. On the contrary, the total relative intensity of CHON compounds significantly increased in winter, mainly composed of nitro compounds or organonitrates. The enhanced formation of nitrophenols in winter indicated the BB influence. The increasing organonitrates formation in winter highlighted the secondary N-containing compounds formation via NO_3 radical-initiated oxidation processes. It is worth noting that the top CHON compounds in summer were referring to reduced N compounds produced from the aldehyde−ammonia reactions. The S-containing compounds were mainly composed of highly oxidized OSs. The monoterpenes derived OSs and long-chain alkanes derived OSs were widely observed in both summer and winter samples, while the aromatic OSs formation were found to be more significant in winter. The presence of long-chain alkanes derived OSs supported the radiocarbon results, proving that the traffic emission was the important fossil sources at the study site. Our results highlighted the equal importance of future reduction in both fossil and non-fossil emissions on atmospheric pollution control.

Acknowledgments

This research was financially supported by the National Natural Science Foundation of China (grant no. 42192512) and the National Natural Science Foundation of China (grant no. 41977305).

References

Aiona, P. K., Luek, J. L., Timko, S. A., Powers, L. C., Gonsior, M., and Nizkorodov, S. A.: Effect of photolysis on absorption and fluorescence spectra of light-absorbing secondary organic aerosols, Acs Earth Space Chem., 2, 235-245, 10.1021/acsearthspacechem.7b00153, 2018.

Altieri, K. E., Seitzinger, S. P., Carlton, A. G., Turpin, B. J., Klein, G. C., and Marshall, A. G.: Oligomers formed through in-cloud methylglyoxal reactions: Chemical composition, properties,

https://doi.org/10.5194/acp-2022-644
Preprint. Discussion started: 4 October 2022

526 and mechanisms investigated by ultra-high resolution FT-ICR mass spectrometry, Atmos.
527 Environ., 42, 1476-1490, 10.1016/j.atmosenv.2007.11.015, 2008.
528 Altieri, K. E., Turpin, B. J., and Seitzinger, S. P.: Oligomers, organosulfates, and nitrooxy
529 organosulfates in rainwater identified by ultra-high resolution electrospray ionization FT-ICR
530 mass spectrometry, Atmos. Chem. Phys., 9, 2533–2542, www.atmos-chem-phys.net/9/2533/2009/,
531 2009.
532 Bao, M., Zhang, Y. L., Cao, F., Lin, Y. C., Hong, Y., Fan, M., Zhang, Y., Yang, X., and Xie, F.:
533 Light absorption and source apportionment of water soluble humic-like substances (HULIS) in
534 $PM_{2.5}$ at Nanjing, China, Environ. Res., 206, 112554, 10.1016/j.envres.2021.112554, 2022.
535 Berndt, T., Mender, B., Scholz, W., Fischer, L., Herrmann, H., Kulmala, M., and Hansel, A.:
536 Accretion product formation from ozonolysis and OH radical reaction of alpha-Pinene:
537 mechanistic insight and the influence of isoprene and ethylene, Environ. Sci. Technol., 52, 11069-
538 11077, 10.1021/acs.est.8b02210, 2018.
539 Bianco, A., Deguillaume, L., Vaitilingom, M., Nicol, E., Baray, J. L., Chaumerliac, N., and
540 Bridoux, M.: Molecular characterization of cloud water samples collected at the Puy de Dome
541 (France) by Fourier transform ion cyclotron resonance mass spectrometry, Environ. Sci. Technol.,
542 52, 10275-10285, 10.1021/acs.est.8b01964, 2018.
543 Bigg, E. K., and Leck, C.: The composition of fragments of bubbles bursting at the ocean surface,
544 J. Geophys. Res., 113, 10.1029/2007jd009078, 2008.
545 Blair, S. L., MacMillan, A. C., Drozd, G. T., Goldstein, A. H., Chu, R. K., Pasa-Tolic, L., Shaw,
546 J. B., Tolic, N., Lin, P., Laskin, J., Laskin, A., and Nizkorodov, S. A.: Molecular characterization
547 of organosulfur compounds in biodiesel and diesel fuel secondary organic aerosol, Environ. Sci.
548 Technol., 51, 119-127, 10.1021/acs.est.6b03304, 2017.
549 Boreddy, S. K. R., Hegde, P., Aswini, A. R., and Aryasree, S.: Chemical characteristics, size
550 distributions, molecular composition, and brown carbon in South Asian outflow to the Indian
551 Ocean, Earth. Space. Sci., 8, 10.1029/2020ea001615, 2021.
552 Brege, M., Paglione, M., Gilardoni, S., Decesari, S., Facchini, M. C., and Mazzoleni, L. R.:
553 Molecular insights on aging and aqueous-phase processing from ambient biomass burning
554 emissions-influenced Po Valley fog and aerosol, Atmos. Chem. Phys., 18, 13197-13214,
555 10.5194/acp-18-13197-2018, 2018.

https://doi.org/10.5194/acp-2022-644
Preprint. Discussion started: 4 October 2022


Atmospheric Chemistry and Physics Discussions

556 Bruggemann, M., Xu, R., Tilgner, A., Kwong, K. C., Mutzel, A., Poon, H. Y., Otto, T., Schaefer,
557 T., Poulain, L., Chan, M. N., and Herrmann, H.: Organosulfates in ambient aerosol: state of
558 knowledge and future research directions on formation, abundance, fate, and importance, Environ.
559 Sci. Technol., 54, 3767-3782, 10.1021/acs.est.9b06751, 2020.
560 Bruns, E. A., Krapf, M., Orasche, J., Huang, Y., Zimmermann, R., Drinovec, L., Močnik, G., El-
561 Haddad, I., Slowik, J. G., Dommen, J., Baltensperger, U., and Prévôt, A. S. H.: Characterization
562 of primary and secondary wood combustion products generated under different burner loads,
563 Atmos. Chem. Phys., 15, 2825-2841, 10.5194/acp-15-2825-2015, 2015.
564 Cai, J., Zeng, X., Zhi, G., Gligorovski, S., Sheng, G., Yu, Z., Wang, X., and Peng, P. a.: Molecular
565 composition and photochemical evolution of water-soluble organic carbon (WSOC) extracted
566 from field biomass burning aerosols using high-resolution mass spectrometry, Atmos. Chem.
567 Phys., 20, 6115-6128, 10.5194/acp-20-6115-2020, 2020.
568 Chen, Q., Ikemori, F., Higo, H., Asakawa, D., and Mochida, M.: Chemical structural
569 characteristics of HULIS and other fractionated organic matter in urban aerosols: results from mass
570 spectral and FT-IR analysis, Environ. Sci. Technol., 50, 1721-1730, 10.1021/acs.est.5b05277,
571 2016.
572 Chung, C. E., Ramanathan, V., and Decremer, D.: Observationally constrained estimates of
573 carbonaceous aerosol radiative forcing, Proc. Natl. Acad. Sci. U. S. A., 109, 11624-11629,
574 10.1073/pnas.1203707109, 2012.
575 Cui, M., Li, C., Chen, Y., Zhang, F., Li, J., Jiang, B., Mo, Y., Li, J., Yan, C., Zheng, M., Xie, Z.,
576 Zhang, G., and Zheng, J.: Molecular characterization of polar organic aerosol constituents in off-
577 road engine emissions using Fourier transform ion cyclotron resonance mass spectrometry (FT-
578 ICR MS): implications for source apportionment, Atmos. Chem. Phys., 19, 13945-13956,
579 10.5194/acp-19-13945-2019, 2019.
580 Daellenbach, K. R., Kourtchev, I., Vogel, A. L., Bruns, E. A., Jiang, J., Petäjä, T., Jaffrezo, J.-L.,
581 Aksoyoglu, S., Kalberer, M., Baltensperger, U., El Haddad, I., and Prévôt, A. S. H.: Impact of
582 anthropogenic and biogenic sources on the seasonal variation in the molecular composition of
583 urban organic aerosols: a field and laboratory study using ultra-high-resolution mass spectrometry,
584 Atmos. Chem. Phys., 19, 5973-5991, 10.5194/acp-19-5973-2019, 2019.
585 De Haan, D. O., Tapavicza, E., Riva, M., Cui, T., Surratt, J. D., Smith, A. C., Jordan, M. C.,
586 Nilakantan, S., Almodovar, M., Stewart, T. N., de Loera, A., De Haan, A. C., Cazaunau, M.,

https://doi.org/10.5194/acp-2022-644
Preprint. Discussion started: 4 October 2022


Atmospheric Chemistry and Physics Discussions

587 Gratien, A., Pangui, E., and Doussin, J. F.: Nitrogen-containing, light-Absorbing oligomers
588 produced in aerosol particles exposed to methylglyoxal, photolysis, and cloud cycling, Environ.
589 Sci. Technol., 52, 4061-4071, 10.1021/acs.est.7b06105, 2018.
590 Fleming, L. T., Lin, P., Roberts, J. M., Selimovic, V., Yokelson, R., Laskin, J., Laskin, A., and
591 Nizkorodov, S. A.: Molecular composition and photochemical lifetimes of brown carbon
592 chromophores in biomass burning organic aerosol, Atmos. Chem. Phys., 20, 1105-1129,
593 10.5194/acp-20-1105-2020, 2020.
594 Glasius, M., Thomsen, D., Wang, K., Iversen, L. S., Duan, J., and Huang, R. J.: Chemical
595 characteristics and sources of organosulfates, organosulfonates, and carboxylic acids in aerosols
596 in urban Xi'an, Northwest China, Sci. Total. Environ., 151187, 10.1016/j.scitotenv.2021.151187,
597 2021.
598 Graber, E. R., and Rudich, Y.: Atmospheric HULIS: How humic-like are they? A comprehensive
599 and critical review, Atmos. Chem. Phys., 6, 729-753, 10.5194/acp-6-729-2006, 2006.
600 Han, H., Feng, Y., Chen, J., Xie, Q., Chen, S., Sheng, M., Zhong, S., Wei, W., Su, S., and Fu, P.:
601 Acidification impacts on the molecular composition of dissolved organic matter revealed by FT-
602 ICR MS, Sci. Total. Environ., 805, 150284, 10.1016/j.scitotenv.2021.150284, 2022.
603 He, Q., Tomaz, S., Li, C., Zhu, M., Meidan, D., Riva, M., Laskin, A., Brown, S. S., George, C.,
604 Wang, X., and Rudich, Y.: Optical properties of secondary organic aerosol produced by nitrate
605 radical oxidation of biogenic volatile organic compounds, Environ. Sci. Technol., 55, 2878-2889,
606 10.1021/acs.est.0c06838, 2021.
607 Huang, L., Liu, T., and Grassian, V. H.: Radical-initiated formation of aromatic organosulfates
608 and sulfonates in the aqueous phase, Environ. Sci. Technol., 54, 11857-11864,
609 10.1021/acs.est.0c05644, 2020.
610 Huang, R.-J., Yang, L., Shen, J., Yuan, W., Gong, Y., Ni, H., Duan, J., Yan, J., Huang, H., You,
611 Q., and Li, Y. J.: Chromophoric fingerprinting of brown carbon from residential biomass burning,
612 Environ. Sci. Technol. Lett., 9, 102-111, 10.1021/acs.estlett.1c00837, 2021.
613 Huo, Y., Guo, Z., Li, Q., Wu, D., Ding, X., Liu, A., Huang, D., Qiu, G., Wu, M., Zhao, Z., Sun,
614 H., Song, W., Li, X., Chen, Y., Wu, T., and Chen, J.: Chemical fingerprinting of HULIS in
615 particulate matters emitted from residential coal and biomass combustion, Environ. Sci. Technol.,
616 55, 3593-3603, 10.1021/acs.est.0c08518, 2021.

https://doi.org/10.5194/acp-2022-644
Preprint. Discussion started: 4 October 2022


Atmospheric Chemistry and Physics Discussions

617 Jang, K. S., Choi, M., Park, M., Park, M. H., Kim, Y. H., Seo, J., Wang, Y., Hu, M., Bae, M. S.,
618 and Park, K.: Assessment of $PM_{2.5}$-bound nitrogen-containing organic compounds (NOCs) during
619 winter at urban sites in China and Korea, Environ. Pollut., 265, 114870,
620 10.1016/j.envpol.2020.114870, 2020.
621 Jiang, B., Liang, Y., Xu, C., Zhang, J., Hu, M., and Shi, Q.: Polycyclic aromatic hydrocarbons
622 (PAHs) in ambient aerosols from Beijing: characterization of low volatile PAHs by positive-ion
623 atmospheric pressure photoionization (APPI) coupled with Fourier transform ion cyclotron
624 resonance, Environ. Sci. Technol., 48, 4716-4723, 10.1021/es405295p, 2014.
625 Jiang, H., Li, J., Chen, D., Tang, J., Cheng, Z., Mo, Y., Su, T., Tian, C., Jiang, B., Liao, Y., and
626 Zhang, G.: Biomass burning organic aerosols significantly influence the light absorption properties
627 of polarity-dependent organic compounds in the Pearl River Delta Region, China, Environ. Int.,
628 144, 106079, 10.1016/j.envint.2020.106079, 2020.
629 Jiang, H., Li, J., Sun, R., Tian, C., Tang, J., Jiang, B., Liao, Y., Chen, C. E., and Zhang, G.:
630 Molecular dynamics and light absorption properties of atmospheric dissolved organic matter,
631 Environ. Sci. Technol., 55, 10268-10279, 10.1021/acs.est.1c01770, 2021.
632 Koch, B. P., and Dittmar, T.: From mass to structure: an aromaticity index for high-resolution
633 mass data of natural organic matter, Rapid. Commun. Mass. Sp., 20, 926-932, 10.1002/rcm.2386,
634 2006.
635 Kourtchev, I., Fuller, S., Aalto, J., Ruuskanen, T. M., McLeod, M. W., Maenhaut, W., Jones, R.,
636 Kulmala, M., and Kalberer, M.: Molecular composition of boreal forest aerosol from Hyytiala,
637 Finland, using ultrahigh resolution mass spectrometry, Environ. Sci. Technol., 47, 4069-4079,
638 10.1021/es3051636, 2013.
639 Kourtchev, I., O'Connor, I. P., Giorio, C., Fuller, S. J., Kristensen, K., Maenhaut, W., Wenger, J.
640 C., Sodeau, J. R., Glasius, M., and Kalberer, M.: Effects of anthropogenic emissions on the
641 molecular composition of urban organic aerosols: An ultrahigh resolution mass spectrometry study,
642 Atmos. Environ., 89, 525-532, 10.1016/j.atmosenv.2014.02.051, 2014.
643 Kourtchev, I., Godoi, R. H. M., Connors, S., Levine, J. G., Archibald, A. T., Godoi, A. F. L.,
644 Paralovo, S. L., Barbosa, C. G. G., Souza, R. A. F., Manzi, A. O., Seco, R., Sjostedt, S., Park, J.-
645 H., Guenther, A., Kim, S., Smith, J., Martin, S. T., and Kalberer, M.: Molecular composition of
646 organic aerosols in central Amazonia: an ultra-high-resolution mass spectrometry study, Atmos.
647 Chem. Phys., 16, 11899-11913, 10.5194/acp-16-11899-2016, 2016.

https://doi.org/10.5194/acp-2022-644
Preprint. Discussion started: 4 October 2022


Atmospheric Chemistry and Physics Discussions

Kroll, J. H., Donahue, N. M., Jimenez, J. L., Kessler, S. H., Canagaratna, M. R., Wilson, K. R., Altieri, K. E., Mazzoleni, L. R., Wozniak, A. S., Bluhm, H., Mysak, E. R., Smith, J. D., Kolb, C. E., and Worsnop, D. R.: Carbon oxidation state as a metric for describing the chemistry of atmospheric organic aerosol, Nat. Chem., 3, 133-139, 10.1038/nchem.948, 2011.

Kuang, B. Y., Lin, P., Huang, X. H. H., and Yu, J. Z.: Sources of humic-like substances in the Pearl River Delta, China: positive matrix factorization analysis of $PM_{2.5}$ major components and source markers, Atmos. Chem. Phys., 15, 1995-2008, 10.5194/acp-15-1995-2015, 2015.

Laskin, A., Smith, J. S., and Laskin, J.: Molecular characterization of nitrogen-containing organic compounds in biomass burning aerosols using high-resolution mass spectrometry, Environ. Sci. Technol., 43, 3764-3771, 10.1021/es803456n, 2009.

Laskin, J., Laskin, A., and Nizkorodov, S. A.: Mass spectrometry analysis in atmospheric chemistry, Anal. Chem., 90, 166-189, 10.1021/acs.analchem.7b04249, 2018.

Levin, I., and Kromer, B.: The tropospheric $^{14}CO_2$ level in mid-latitudes of the northern hemisphere (1959–2003), Radiocarbon, 46, 1261-1272, 10.1017/s0033822200033130, 2004.

Levin, I., Kromer, B., and Hammer, S.: Atmospheric $\Delta^{14}CO_2$ trend in Western European background air from 2000 to 2012, Tellus. B., 65, 10.3402/tellusb.v65i0.20092, 2013.

Li, X., Han, J., Hopke, P. K., Hu, J., Shu, Q., Chang, Q., and Ying, Q.: Quantifying primary and secondary humic-like substances in urban aerosol based on emission source characterization and a source-oriented air quality model, Atmos. Chem. Phys., 19, 2327-2341, 10.5194/acp-19-2327-2019, 2019.

Li, X., Yu, F., Cao, J., Fu, P., Hua, X., Chen, Q., Li, J., Guan, D., Tripathee, L., Chen, Q., and Wang, Y.: Chromophoric dissolved organic carbon cycle and its molecular compositions and optical properties in precipitation in the Guanzhong basin, China, Sci. Total. Environ., 814, 152775, 10.1016/j.scitotenv.2021.152775, 2022.

Lin, P., Rincon, A. G., Kalberer, M., and Yu, J. Z.: Elemental composition of HULIS in the Pearl River Delta Region, China: results inferred from positive and negative electrospray high resolution mass spectrometric data, Environ. Sci. Technol., 46, 7454-7462, 10.1021/es300285d, 2012a.

Lin, P., Yu, J. Z., Engling, G., and Kalberer, M.: Organosulfates in humic-like substance fraction isolated from aerosols at seven locations in East Asia: a study by ultra-high-resolution mass spectrometry, Environ. Sci. Technol., 46, 13118-13127, 10.1021/es303570v, 2012b.

https://doi.org/10.5194/acp-2022-644
Preprint. Discussion started: 4 October 2022


Atmospheric Chemistry and Physics Discussions

678 Lin, P., Aiona, P. K., Li, Y., Shiraiwa, M., Laskin, J., Nizkorodov, S. A., and Laskin, A.: Molecular
679 characterization of brown carbon in biomass burning aerosol particles, Environ. Sci. Technol., 50,
680 11815-11824, 10.1021/acs.est.6b03024, 2016.
681 Lin, P., Bluvshtein, N., Rudich, Y., Nizkorodov, S. A., Laskin, J., and Laskin, A.: Molecular
682 chemistry of atmospheric brown carbon inferred from a nationwide biomass burning event,
683 Environ. Sci. Technol., 51, 11561-11570, 10.1021/acs.est.7b02276, 2017.
684 Lin, P., Fleming, L. T., Nizkorodov, S. A., Laskin, J., and Laskin, A.: Comprehensive molecular
685 characterization of atmospheric brown carbon by high resolution mass spectrometry with
686 electrospray and atmospheric pressure photoionization, Anal. Chem., 90, 12493-12502,
687 10.1021/acs.analchem.8b02177, 2018.
688 Liu, X., Zhang, Y.-L., Peng, Y., Xu, L., Zhu, C., Cao, F., Zhai, X., Haque, M. M., Yang, C., Chang,
689 Y., Huang, T., Xu, Z., Bao, M., Zhang, W., Fan, M., and Lee, X.: Chemical and optical properties
690 of carbonaceous aerosols in Nanjing, eastern China: regionally transported biomass burning
691 contribution, Atmos. Chem. Phys., 19, 11213-11233, 10.5194/acp-19-11213-2019, 2019.
692 Ma, L., Li, B., Liu, Y., Sun, X., Fu, D., Sun, S., Thapa, S., Geng, J., Qi, H., Zhang, A., and Tian,
693 C.: Characterization, sources and risk assessment of $PM_{2.5}$-bound polycyclic aromatic
694 hydrocarbons (PAHs) and nitrated PAHs (NPAHs) in Harbin, a cold city in Northern China, J.
695 Clean. Prod., 264, 10.1016/j.jclepro.2020.121673, 2020.
696 Ma, Y., Cheng, Y., Qiu, X., Cao, G., Fang, Y., Wang, J., Zhu, T., Yu, J., and Hu, D.: Sources and
697 oxidative potential of water-soluble humic-like substances ($HULIS_{WS}$) in fine particulate matter
698 ($PM_{2.5}$) in Beijing, Atmos. Chem. Phys., 18, 5607-5617, 10.5194/acp-18-5607-2018, 2018.
699 Mo, Y., Li, J., Jiang, B., Su, T., Geng, X., Liu, J., Jiang, H., Shen, C., Ding, P., Zhong, G., Cheng,
700 Z., Liao, Y., Tian, C., Chen, Y., and Zhang, G.: Sources, compositions, and optical properties of
701 humic-like substances in Beijing during the 2014 APEC summit: Results from dual carbon isotope
702 and Fourier-transform ion cyclotron resonance mass spectrometry analyses, Environ. Pollut., 239,
703 322-331, 10.1016/j.envpol.2018.04.041, 2018.
704 Mohr, C., Lopez-Hilfiker, F. D., Zotter, P., Prevot, A. S., Xu, L., Ng, N. L., Herndon, S. C.,
705 Williams, L. R., Franklin, J. P., Zahniser, M. S., Worsnop, D. R., Knighton, W. B., Aiken, A. C.,
706 Gorkowski, K. J., Dubey, M. K., Allan, J. D., and Thornton, J. A.: Contribution of nitrated phenols
707 to wood burning brown carbon light absorption in Detling, United Kingdom during winter time,
708 Environ. Sci. Technol., 47, 6316-6324, 10.1021/es400683v, 2013.

https://doi.org/10.5194/acp-2022-644
Preprint. Discussion started: 4 October 2022


Atmospheric Chemistry and Physics Discussions

709 Mutzel, A., Poulain, L., Berndt, T., Iinuma, Y., Rodigast, M., Boge, O., Richters, S., Spindler, G.,
710 Sipila, M., Jokinen, T., Kulmala, M., and Herrmann, H.: Highly oxidized multifunctional organic
711 compounds observed in tropospheric particles: a field and laboratory study, Environ. Sci. Technol.,
712 49, 7754-7761, 10.1021/acs.est.5b00885, 2015.
713 Ning, C., Gao, Y., Zhang, H., Yu, H., Wang, L., Geng, N., Cao, R., and Chen, J.: Molecular
714 characterization of dissolved organic matters in winter atmospheric fine particulate matters ($PM_{2.5}$)
715 from a coastal city of northeast China, Sci. Total. Environ., 689, 312-321,
716 10.1016/j.scitotenv.2019.06.418, 2019.
717 Ning, C., Gao, Y., Yu, H., Zhang, H., Geng, N., Cao, R., and Chen, J.: FT-ICR mass spectrometry
718 for molecular characterization of water-insoluble organic compounds in winter atmospheric fine
719 particulate matters, J. Environ. Sci., 111, 51-60, 10.1016/j.jes.2020.12.017, 2022.
720 Noziere, B., Kalberer, M., Claeys, M., Allan, J., D'Anna, B., Decesari, S., Finessi, E., Glasius, M.,
721 Grgic, I., Hamilton, J. F., Hoffmann, T., Iinuma, Y., Jaoui, M., Kahnt, A., Kampf, C. J., Kourtchev,
722 I., Maenhaut, W., Marsden, N., Saarikoski, S., Schnelle-Kreis, J., Surratt, J. D., Szidat, S.,
723 Szmigielski, R., and Wisthaler, A.: The molecular identification of organic compounds in the
724 atmosphere: state of the art and challenges, Chem. Rev., 115, 3919-3983, 10.1021/cr5003485,
725 2015.
726 O'Brien, R. E., Laskin, A., Laskin, J., Rubitschun, C. L., Surratt, J. D., and Goldstein, A. H.:
727 Molecular characterization of S- and N-containing organic constituents in ambient aerosols by
728 negative ion mode high-resolution Nanospray desorption electrospray ionization mass
729 spectrometry: CalNex 2010 field study, J. Geophy. Res. -Atmos., 119, 10.1002/2014jd021955,
730 2014.
731 Patriarca, C., Bergquist, J., Sjoberg, P. J. R., Tranvik, L., and Hawkes, J. A.: Online HPLC-ESI-
732 HRMS method for the analysis and comparison of different dissolved organic matter samples,
733 Environ. Sci. Technol., 52, 2091-2099, 10.1021/acs.est.7b04508, 2018.
734 Pospisilova, V., Lopez-Hilfiker, F. D., Bell, D. M., Haddad, I. E., Mohr, C., Huang, W., Heikkinen,
735 L., Xiao, M., Dommen, J., Prevot, A. S. H., Baltensperger, U., and Slowik, J. G.: On the fate of
736 oxygenated organic molecules in atmospheric aerosol particles, Sci. Adv., 6, 2020.
737 Qi, L., Zhang, Z., Wang, X., Deng, F., Zhao, J., and Liu, H.: Molecular characterization of
738 atmospheric particulate organosulfates in a port environment using ultrahigh resolution mass

https://doi.org/10.5194/acp-2022-644
Preprint. Discussion started: 4 October 2022


Atmospheric Chemistry and Physics Discussions

739 spectrometry: Identification of traffic emissions, J. Hazard. Mater., 419, 126431,
740 10.1016/j.jhazmat.2021.126431, 2021.
741 Riva, M., Tomaz, S., Cui, T., Lin, Y.-H., Perraudin, E., Gold, A., Stone, E. A., Villenave, E., and
742 Surratt, J. D.: Evidence for an unrecognized secondary anthropogenic source of organosulfates and
743 sulfonates: gas-phase oxidation of polycyclic aromatic hydrocarbons in the presence of sulfate
744 aerosol, Environ. Sci. Technol., 49, 6654-6664, 10.1021/acs.est.5b00836, 2015.
745 Shen, H., Zhao, D., Pullinen, I., Kang, S., Vereecken, L., Fuchs, H., Acir, I. H., Tillmann, R.,
746 Rohrer, F., Wildt, J., Kiendler-Scharr, A., Wahner, A., and Mentel, T. F.: Highly oxygenated
747 organic nitrates formed from NO_3 radical-initiated oxidation of beta-Pinene, Environ. Sci.
748 Technol., 10.1021/acs.est.1c03978, 2021.
749 Siemens, K., Morales, A., He, Q., Li, C., Hettiyadura, A. P. S., Rudich, Y., and Laskin, A.:
750 Molecular analysis of secondary brown carbon produced from the photooxidation of naphthalene,
751 Environ. Sci. Technol., 2022.
752 Song, J., Li, M., Jiang, B., Wei, S., Fan, X., and Peng, P.: Molecular characterization of water-
753 soluble humic like substances in smoke particles emitted from combustion of biomass materials
754 and coal using Ultrahigh-resolution electrospray ionization fourier transform ion cyclotron
755 resonance mass spectrometry, Environ. Sci. Technol., 52, 2575-2585, 10.1021/acs.est.7b06126,
756 2018.
757 Song, J., Li, M., Fan, X., Zou, C., Zhu, M., Jiang, B., Yu, Z., Jia, W., Liao, Y., and Peng, P.:
758 Molecular characterization of water- and methanol-soluble organic compounds emitted from
759 residential coal combustion using Ultrahigh-resolution electrospray ionization fourier transform
760 ion cyclotron resonance mass spectrometry, Environ. Sci. Technol., 53, 13607-13617,
761 10.1021/acs.est.9b04331, 2019.
762 Song, J., Li, M., Zou, C., Cao, T., Fan, X., Jiang, B., Yu, Z., Jia, W., and Peng, P.: Molecular
763 characterization of nitrogen-containing compounds in humic-like substances emitted from
764 biomass burning and coal combustion, Environ. Sci. Technol., 56, 119-130,
765 10.1021/acs.est.1c04451, 2022.
766 Sun, H., Li, X., Zhu, C., Huo, Y., Zhu, Z., Wei, Y., Yao, L., Xiao, H., and Chen, J.: Molecular
767 composition and optical property of humic-like substances (HULIS) in winter-time $PM_{2.5}$ in the
768 rural area of North China Plain, Atmos. Environ., 252, 10.1016/j.atmosenv.2021.118316, 2021.

https://doi.org/10.5194/acp-2022-644
Preprint. Discussion started: 4 October 2022


Atmospheric Chemistry and Physics Discussions

769 Surratt, J. D., Go´mez-Gonza´lez, Y., Chan, A. W. H., Vermeylen, R., Shahgholi, M., Kleindienst,
770 T. E., Edney, E. O., Offenberg, J. H., Lewandowski, M., Jaoui, M., Maenhaut, W., Claeys, M.,
771 Flagan, R. C., and Seinfeld, J. H.: Organosulfate formation in biogenic secondary organic aerosol,
772 J. Phys. Chem. A 112, 8345-8378, 10.1021/jp802310p, 2008.
773 Tang, J., Li, J., Su, T., Han, Y., Mo, Y., Jiang, H., Cui, M., Jiang, B., Chen, Y., Tang, J., Song, J.,
774 Peng, P. a., and Zhang, G.: Molecular compositions and optical properties of dissolved brown
775 carbon in biomass burning, coal combustion, and vehicle emission aerosols illuminated by
776 excitation–emission matrix spectroscopy and Fourier transform ion cyclotron resonance mass
777 spectrometry analysis, Atmos. Chem. Phys., 20, 2513-2532, 10.5194/acp-20-2513-2020, 2020.
778 Tao, S., Lu, X., Levac, N., Bateman, A. P., Nguyen, T. B., Bones, D. L., Nizkorodov, S. A., Laskin,
779 J., Laskin, A., and Yang, X.: Molecular characterization of organosulfates in organic aerosols from
780 Shanghai and Los Angeles urban areas by nanospray-desorption electrospray ionization high-
781 resolution mass spectrometry, Environ. Sci. Technol., 48, 10993-11001, 10.1021/es5024674, 2014.
782 Tsui, W. G., and McNeill, V. F.: Modeling secondary organic aerosol production from
783 photosensitized humic-like substances (HULIS), Environ. Sci. Technol. Lett., 5, 255-259,
784 10.1021/acs.estlett.8b00101, 2018.
785 Wang, K., Zhang, Y., Huang, R.-J., Cao, J., and Hoffmann, T.: UHPLC-Orbitrap mass
786 spectrometric characterization of organic aerosol from a central European city (Mainz, Germany)
787 and a Chinese megacity (Beijing), Atmos. Environ., 189, 22-29, 10.1016/j.atmosenv.2018.06.036,
788 2018a.
789 Wang, K., Zhang, Y., Huang, R. J., Wang, M., Ni, H., Kampf, C. J., Cheng, Y., Bilde, M., Glasius,
790 M., and Hoffmann, T.: Molecular characterization and source identification of atmospheric
791 particulate organosulfates using ultrahigh resolution mass spectrometry, Environ. Sci. Technol.,
792 53, 6192-6202, 10.1021/acs.est.9b02628, 2019a.
793 Wang, X., Hayeck, N., Brüggemann, M., Yao, L., Chen, H., Zhang, C., Emmelin, C., Chen, J.,
794 George, C., and Wang, L.: Chemical characteristics of organic aerosols in Shanghai: a Study by
795 Ultrahigh-performance liquid chromatography coupled with orbitrap mass spectrometry, J.
796 Geophys. Res. -Atmos., 122, 11,703-711,722, 10.1002/2017jd026930, 2017a.
797 Wang, X., Heald, C. L., Liu, J., Weber, R. J., Campuzano-Jost, P., Jimenez, J. L., Schwarz, J. P.,
798 and Perring, A. E.: Exploring the observational constraints on the simulation of brown carbon,
799 Atmos. Chem. Phys., 18, 635-653, 10.5194/acp-18-635-2018, 2018b.

https://doi.org/10.5194/acp-2022-644
Preprint. Discussion started: 4 October 2022


Atmospheric Chemistry and Physics Discussions

800 Wang, X. K., Rossignol, S., Ma, Y., Yao, L., Wang, M. Y., Chen, J. M., George, C., and Wang,
801 L.: Molecular characterization of atmospheric particulate organosulfates in three megacities at the
802 middle and lower reaches of the Yangtze River, Atmos. Chem. Phys., 16, 2285-2298, 10.5194/acp-
803 16-2285-2016, 2016.
804 Wang, Y., Hu, M., Lin, P., Guo, Q., Wu, Z., Li, M., Zeng, L., Song, Y., Zeng, L., Wu, Y., Guo, S.,
805 Huang, X., and He, L.: Molecular characterization of nitrogen-containing organic compounds in
806 humic-like substances emitted from straw residue burning, Environ. Sci. Technol., 51, 5951-5961,
807 10.1021/acs.est.7b00248, 2017b.
808 Wang, Y., Hu, M., Guo, S., Wang, Y., Zheng, J., Yang, Y., Zhu, W., Tang, R., Li, X., Liu, Y., Le
809 Breton, M., Du, Z., Shang, D., Wu, Y., Wu, Z., Song, Y., Lou, S., Hallquist, M., and Yu, J.: The
810 secondary formation of organosulfates under interactions between biogenic emissions and
811 anthropogenic pollutants in summer in Beijing, Atmos. Chem. Phys., 18, 10693-10713,
812 10.5194/acp-18-10693-2018, 2018c.
813 Wang, Y., Hu, M., Lin, P., Tan, T., Li, M., Xu, N., Zheng, J., Du, Z., Qin, Y., Wu, Y., Lu, S., Song,
814 Y., Wu, Z., Guo, S., Zeng, L., Huang, X., and He, L.: Enhancement in particulate organic nitrogen
815 and light absorption of humic-like substances over Tibetan Plateau due to long-range transported
816 biomass burning emissions, Environ. Sci. Technol., 53, 14222-14232, 10.1021/acs.est.9b06152,
817 2019b.
818 Wang, Y., Hu, M., Wang, Y.-C., Li, X., Fang, X., Tang, R., Lu, S., Wu, Y., Guo, S., Wu, Z.,
819 Hallquist, M., and Yu, J. Z.: Comparative study of particulate organosulfates in contrasting
820 atmospheric environments: field evidence for the significant influence of anthropogenic sulfate
821 and NO_x, Environ. Sci. Technol. Lett., 7, 787-794, 10.1021/acs.estlett.0c00550, 2020.
822 Willoughby, A. S., Wozniak, A. S., and Hatcher, P. G.: A molecular-level approach for
823 characterizing water-insoluble components of ambient organic aerosol particulates using
824 ultrahigh-resolution mass spectrometry, Atmos. Chem. Phys., 14, 10299-10314, 10.5194/acp-14-
825 10299-2014, 2014.
826 Wozniak, A. S., Bauer, J. E., Sleighter, R. L., Dickhut, R. M., and Hatcher, P. G.: Technical note:
827 Molecular characterization of aerosol-derived water soluble organic carbon using ultrahigh
828 resolution electrospray ionization Fourier transform ion cyclotron resonance mass spectrometry,
829 Atmos. Chem. Phys., 8, 5099–5111, www.atmos-chem-phys.net/8/5099/2008/, 2008.

https://doi.org/10.5194/acp-2022-644
Preprint. Discussion started: 4 October 2022


Atmospheric Chemistry and Physics Discussions

Wu, C., Yang, J., Fu, Q., Zhu, B., Ruan, T., and Jiang, G.: Molecular characterization of water-soluble organic compounds in $PM_{2.5}$ using ultrahigh resolution mass spectrometry, Sci. Total. Environ., 668, 917-924, 10.1016/j.scitotenv.2019.03.031, 2019a.

Wu, G., Ram, K., Fu, P., Wang, W., Zhang, Y., Liu, X., Stone, E. A., Pradhan, B. B., Dangol, P. M., Panday, A. K., Wan, X., Bai, Z., Kang, S., Zhang, Q., and Cong, Z.: Water-soluble brown carbon in atmospheric aerosols from Godavari (Nepal), a regional representative of South Asia, Environ. Sci. Technol., 53, 3471-3479, 10.1021/acs.est.9b00596, 2019b.

Xie, M., Chen, X., Hays, M. D., Lewandowski, M., Offenberg, J., Kleindienst, T. E., and Holder, A. L.: Light absorption of secondary organic aerosol: composition and contribution of nitroaromatic compounds, Environ. Sci. Technol., 51, 11607-11616, 10.1021/acs.est.7b03263, 2017.

Yang, Z., Tsona, N. T., Li, J., Wang, S., Xu, L., You, B., and Du, L.: Effects of NO_x and SO_2 on the secondary organic aerosol formation from the photooxidation of 1,3,5-trimethylbenzene: A new source of organosulfates, Environ. Pollut., 264, 114742, 10.1016/j.envpol.2020.114742, 2020.

Yang, Z., Tsona, N. T., George, C., and Du, L.: Nitrogen-containing compounds enhance Light absorption of aromatic-derived brown carbon, Environ. Sci. Technol., 10.1021/acs.est.1c08794, 2022.

Zhang, A., Wang, Y., Zhang, Y., Weber, R. J., Song, Y., Ke, Z., and Zou, Y.: Modeling the global radiative effect of brown carbon: a potentially larger heating source in the tropical free troposphere than black carbon, Atmos. Chem. Phys., 20, 1901-1920, 10.5194/acp-20-1901-2020, 2020.

Zhang, R., Gen, M., Liang, Z., Li, Y. J., and Chan, C. K.: Photochemical reactions of glyoxal during particulate ammonium nitrate photolysis: brown carbon formation, enhanced glyoxal decay, and organic phase formation, Environ. Sci. Technol., 56, 1605-1614, 10.1021/acs.est.1c07211, 2022.

Zhang, Y., Forrister, H., Liu, J., Dibb, J., Anderson, B., Schwarz, J. P., Perring, A. E., Jimenez, J. L., Campuzano-Jost, P., Wang, Y., Nenes, A., and Weber, R. J.: Top-of-atmosphere radiative forcing aected by brown carbon in the upper troposphere, Nat. Geosci., 10, 486-489, 10.1038/NGEO2960, 2017.

Zhao, Y., Hallar, A. G., and Mazzoleni, L. R.: Atmospheric organic matter in clouds: exact masses and molecular formula identification using ultrahigh-resolution FT-ICR mass spectrometry, Atmos. Chem. Phys., 13, 12343-12362, 10.5194/acp-13-12343-2013, 2013.

https://doi.org/10.5194/acp-2022-644
Preprint. Discussion started: 4 October 2022

Atmospheric Chemistry and Physics Discussions

Zheng, G., He, K., Duan, F., Cheng, Y., and Ma, Y.: Measurement of humic-like substances in aerosols: A review, Environ. Pollut., 181, 301-314, 10.1016/j.envpol.2013.05.055, 2013.

Zheng, Y., Chen, Q., Cheng, X., Mohr, C., Cai, J., Huang, W., Shrivastava, M., Ye, P., Fu, P., Shi, X., Ge, Y., Liao, K., Miao, R., Qiu, X., Koenig, T. K., and Chen, S.: Precursors and pathways leading to enhanced secondary organic aerosol formation during severe haze episodes, Environ. Sci. Technol., 10.1021/acs.est.1c04255, 2021.

https://doi.org/10.5194/acp-2022-644
Preprint. Discussion started: 4 October 2022

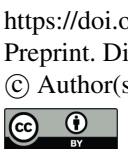

Atmospheric Chemistry and Physics Discussions

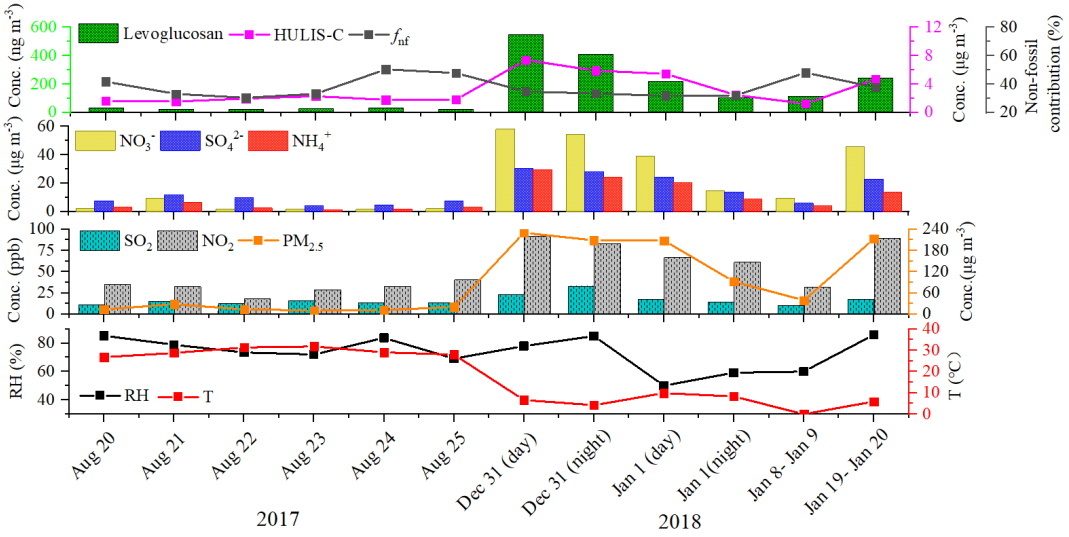

867

868 Figure 1. Time series of non-fossil contributions to HULIS-C, the mass concentrations of HULIS-
869 C, Levoglucosan, NO_3^-, SO_4^{2-}, NH_4^+, SO_2, NO_2, and $PM_{2.5}$, relative humidity, and temperature
870 during the study periods.

https://doi.org/10.5194/acp-2022-644
Preprint. Discussion started: 4 October 2022

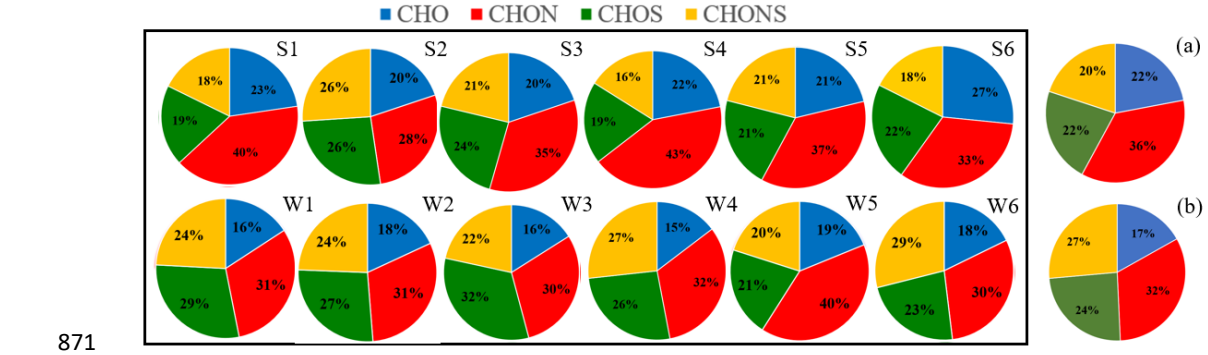

Figure 2. Pie graph of the number percentages of each elemental formula group for the 12 samples plotted in the box and the averaged number percentages of each elemental formula group for the summer samples (a) and winter samples (b).

https://doi.org/10.5194/acp-2022-644
Preprint. Discussion started: 4 October 2022

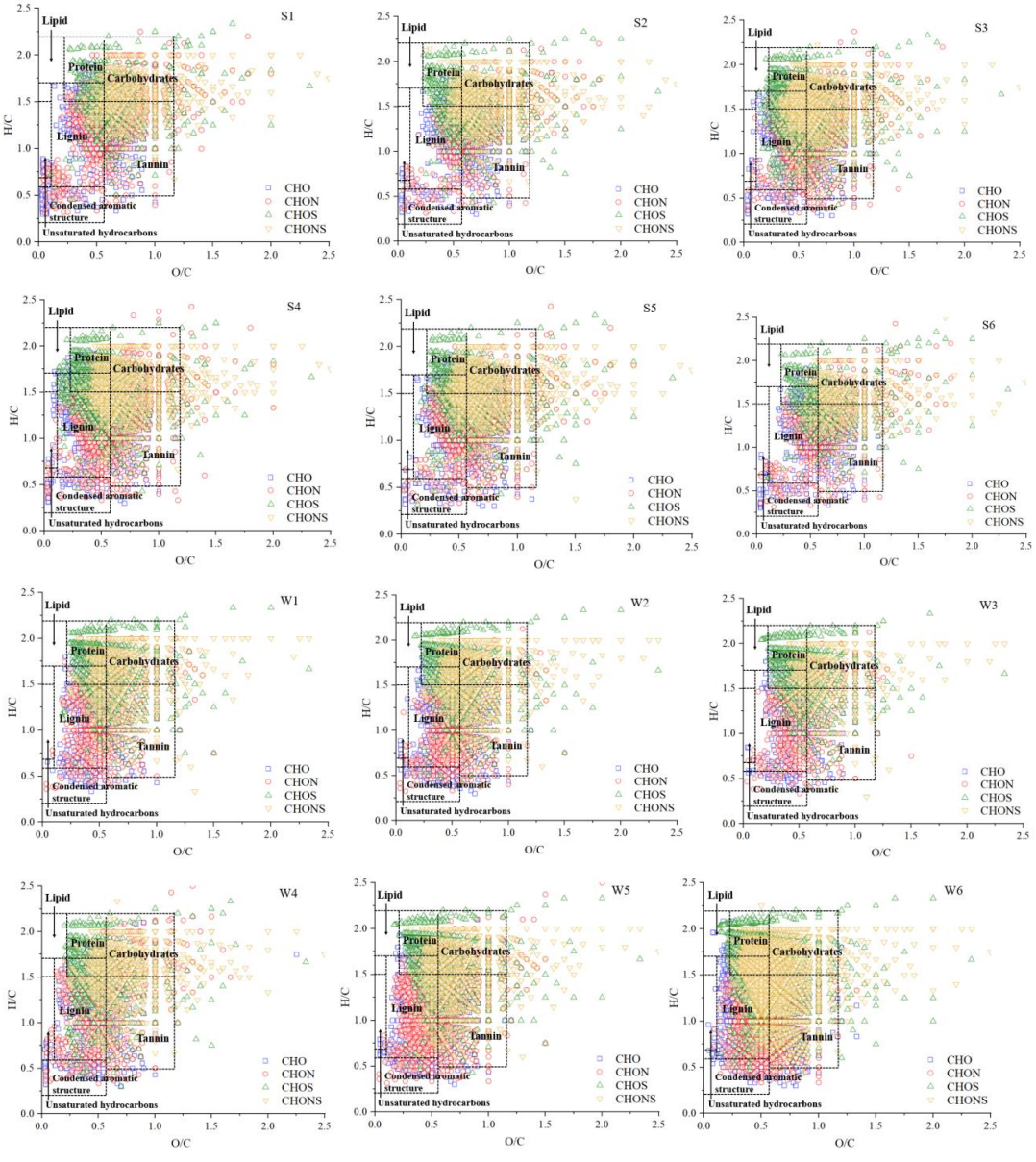

Figure 3. Van Krevelen diagrams of the 12 samples.

https://doi.org/10.5194/acp-2022-644
Preprint. Discussion started: 4 October 2022

Atmospheric Chemistry and Physics Discussions

880

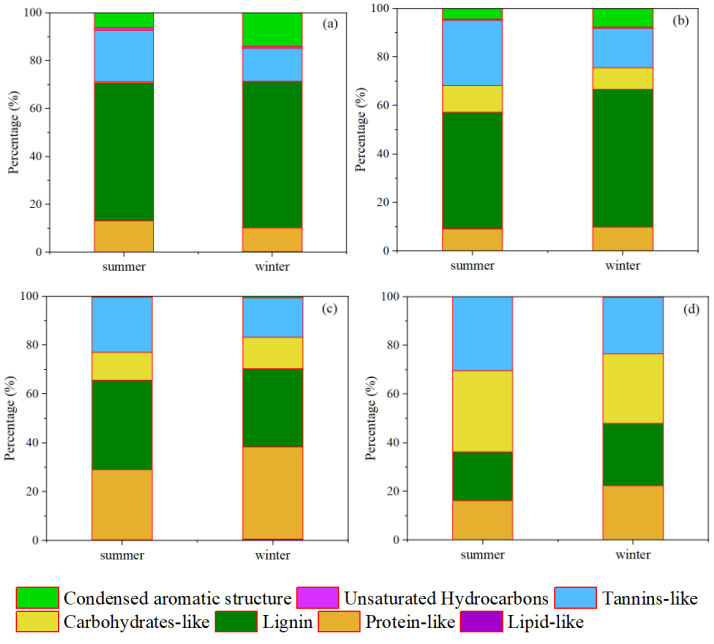

881

882

883 Figure 4. Contributions of seven categories in CHO (a), CHON (b), CHOS (c), and CHONS (d)

884 compounds.

https://doi.org/10.5194/acp-2022-644
Preprint. Discussion started: 4 October 2022

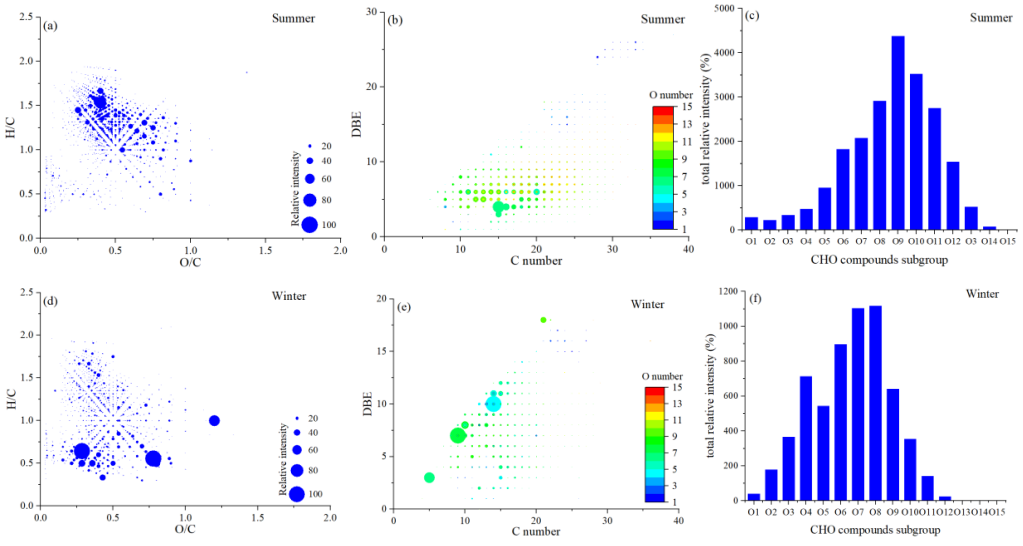

Figure 5. Van Krevelen diagram ((a) and (d)), plot of DBE values vs carbon atom numbers ((b) and (e)), and the total relative intensity of each subgroup ((c) and (f)) for the CHO compounds in summer and winter.

https://doi.org/10.5194/acp-2022-644
Preprint. Discussion started: 4 October 2022

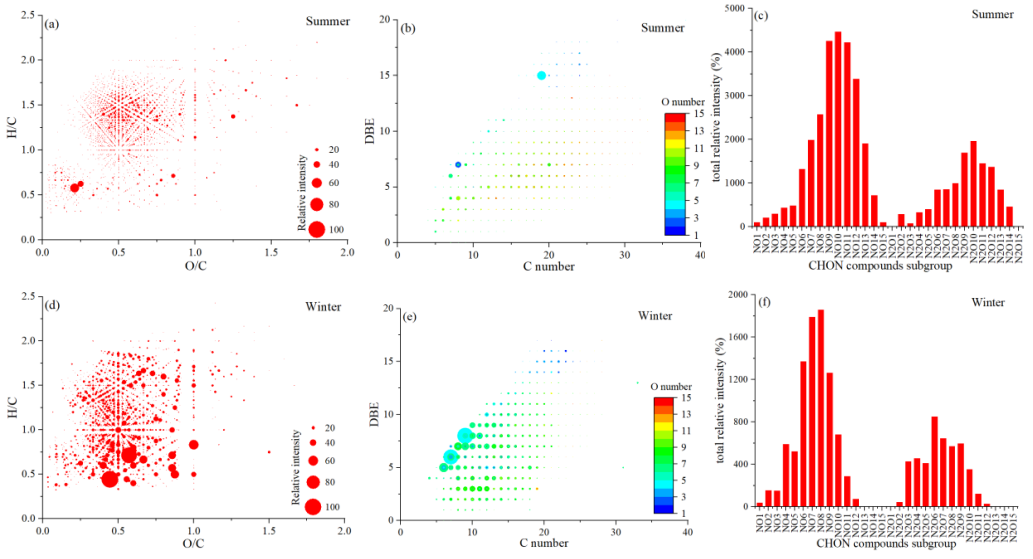

Figure 6. Van Krevelen diagram ((a) and (d)), plot of DBE values vs carbon atom numbers ((b) and (e)), and the total relative intensity of each subgroup ((c) and (f)) for the CHON compounds in summer and winter.

https://doi.org/10.5194/acp-2022-644
Preprint. Discussion started: 4 October 2022

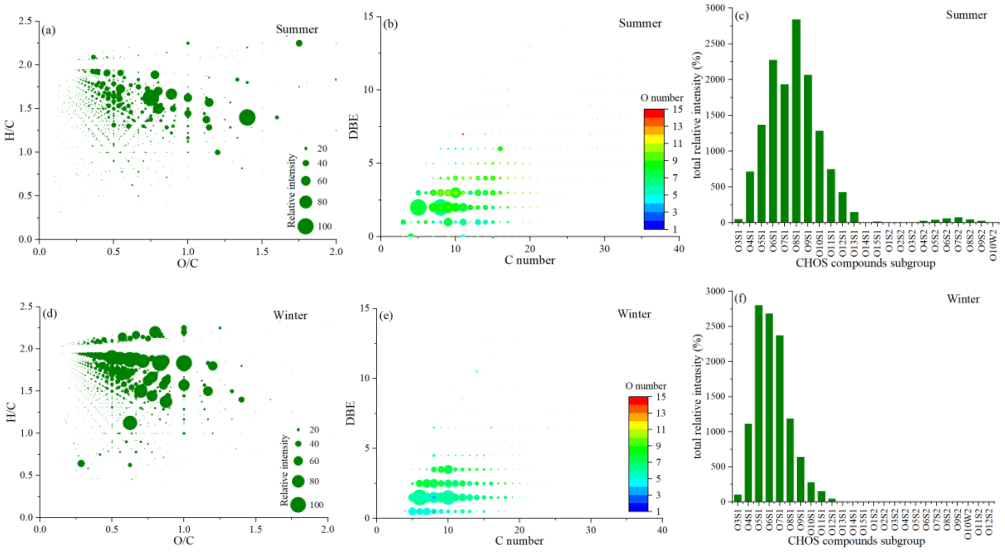

Figure 7. Van Krevelen diagram ((a) and (d)) , plot of DBE values vs carbon atom numbers ((b) and (e)), and the total relative intensity of each subgroup ((c) and (f)) for the CHOS compounds in summer and winter.

https://doi.org/10.5194/acp-2022-644
Preprint. Discussion started: 4 October 2022

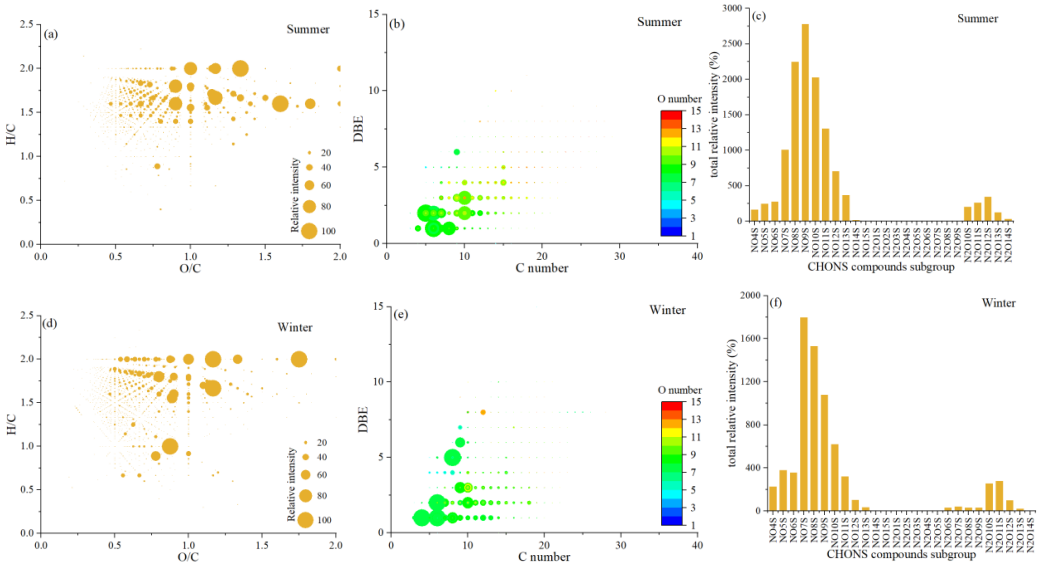

Figure 8. Van Krevelen diagram ((a) and (d)), plot of DBE values vs carbon atom numbers ((b) and (e)), and the total relative intensity of each subgroup ((c) and (f)) for the CHONS compounds in summer and winter.

https://doi.org/10.5194/acp-2022-644
Preprint. Discussion started: 4 October 2022

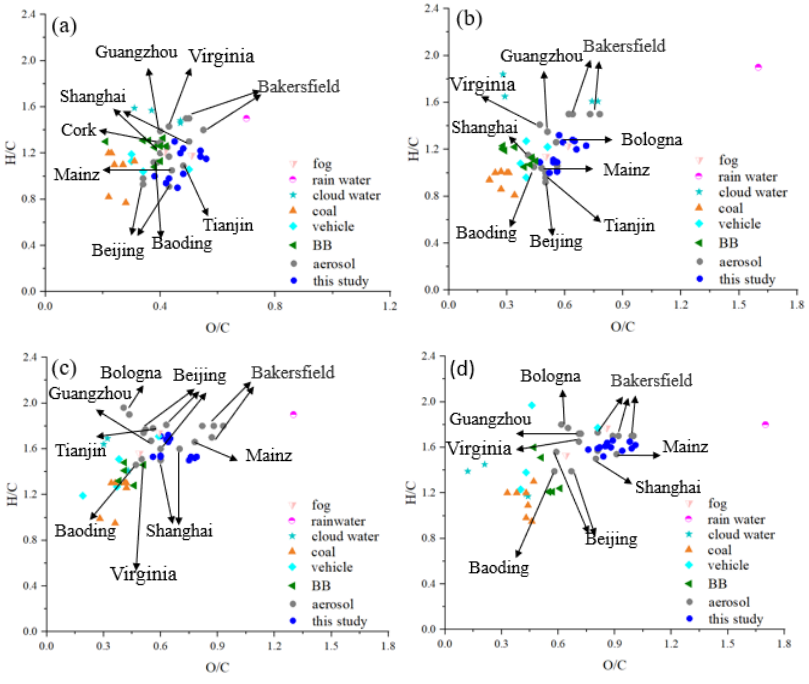

Figure 9. Comparison of O/C and H/C ratios of water soluble organic compounds in different atmospheric media in CHO (a), CHON (b), CHOS (c), and CHONS (d) compounds.